Disclaimer

This note has not been internally reviewed by the DØ Collaboration. Results or plots contained in this note were only intended for internal documentation by the authors of the note and they are not approved as scientific results by either the authors or the DØ Collaboration. All approved scientific results of the DØ Collaboration have been published as internally reviewed Conference Notes or in peer reviewed journals.

DØ Note: 2978
Dec 12th, 1995

Measurement of the Top quark production cross section using *lepton* + jets events

J. M. Butler, S. Chopra, W. Cobau, H. Greenlee, J. Hobbs
M. Narain, S. Protopopescu, T. Rockwell, P. Tamburello, H. Zhu

the DØ Top Lepton+jets Group

1 Introduction

In this note we present an updated analysis of $t\bar{t} \rightarrow$ *lepton*+jet modes which contribute to the measurement of the top production cross section. The data set used for these measurements corresponds to approximately 100 pb^{-1}, almost the entire data sample collected during Run IA and Run IB.

In $t\bar{t}$ decays, we classify events as *lepton*+jets events, if one W decays leptonically to $e\nu$ or $\mu\nu$ and the other hadronically. The branching fraction is 24/81. The dominant source of background for this mode is W+jets production. We further distinguish the b tagged lepton+jets channel, in which a muon from the semileptonic decay of a b quark was detected (ℓ+jets/μ), and the topological lepton+jets channel, in which the topology of the event is top-like and no b was tagged (ℓ+jets.).

2 Luminosity

We used the GET_FILE_LUM utility to obtain the luminosity corresponding to the streamed data sets used for the analyses, this is labled as "RAW" lum in table 1. To get the luminosity for the GOOD_BEAM running condition we apply a correction for MICRO_BLANK, which is taken from the production database and is denoted as "Microblanked". Table 1 also lists the luminosities as a function of Pre and Post muon chamber zap running conditions during Run1B.

In order to compute the luminosity for the MAX_LIVE condition, we used GET_FILT_LUM utility and the ELE_JET_HIGH filter for Run1B.

All of these have to be corrected by a factor of 1.03 to account for the change in min-bias cross section.

A log file with the details can be found in
TOP2$HROOT:[EVENT_SAMPLE.COM.LUM.TOM]AAA-LOG.TXT

3 Data Streaming

For the $lepton + jets$ analyses, we ran over the entire MDS and MDC sample from Run1B (and only $e + jets$ for Run1A) to create smaller event samples which could be located on the top project disks on the Alpha cluster or FNALD0 cluster. These streamed data sets are the starting points for all $lepton + jets$ analyses.

We eventually kept only the samples for signal analysis on disk. The background streams were analyzed and copied off to tape. We streamed all MDS and MDC files available until 24th October, 1995 in the DØ$DATA$DST area.

A document with detailed description of these streams can be found in
TOP_DOC$HROOT:[GENERAL_INFO.EVENT_SAMPLE] RESTREAM_SELECTION.TXT

4 Event Cleanup

We reject runs which have known detector problems or pathologies. These runs are listed in D0$PHYSICS_UTIL$GENERAL:BAD_RUN.RCP. A document describing how the decision was taken to classify these runs as bad can be found in TOP_DOC$HROOT:[GENERAL_INFO.RUN1B]BAD_RUN.MEM

Table 1: Luminosity in pb^{-1} used in *lepton + jet* analyses. The error on the luminosity is 5.4%

	Run1A		
e+jets RAW	14.4		
e+jets Microblanked	13.9		
μ+jets Microblanked	9.8		
	Run1B	Prezap	Postzap
Raw	81.132	48.438	32.694
Remove bad runs - used BAD_RUN.RCP			
Good raw:	80.164	47.879	32.285
Microblanked:	74.863	45.040	29.823
Remove bad runs (ignore muon system) - used BAD_RUN_CAL.RCP			
Good raw cal:	80.226		
Cal microblanked:	74.921		
Remove bad runs - used BAD_RUN.RCP			
MAX_LIVE	88.369	35.877	52.492

We also reject events which are determined to be pathological. If the difference between the CH-fraction and EM-fraction of any jet in the event is more than 0.5, then the event is classified as "BAD" and rejected from the analysis (see figure 1).

We use the routine D0$PHYSICS_UTIL$GENERAL:TOP_EVENT_CLEANUP.FOR for this purpose.

5 Particle Identification

5.1 Electron-id

In the present analysis, we have swicthed to using Electron identification based on a likelihood technique. Details of this method can be found elsewhere[1]. We use the Electron-likelihood variable computed using 4 variables. These variables are

$$\chi^2, \qquad \mathrm{em-fraction}, \qquad \sigma_{trk} \text{ and } \qquad \mathrm{dE/dx}$$

The cut values for the 4-variable electron-likelihood and isolation parameter are listed below :

- CC : elike$\leq$ 0.25 (tight); $\leq$ 0.5 (loose)
- EC : elike$\leq$ 0.30 (tight); $\leq$ 0.5 (loose)
- isolation fraction $\leq$ 0.1

The cut points for the 4-variable electron-likelihood are chosen so as to obtain the same "tight" electron efficiency as we had during the **discovery analysis** ("old") with better rejection against $fake-electron$ backgrounds. This can be seen from table 2, where the efficiencies and rejections of the "old" and "new" electron-id are compared. In this comparion the efficiencies are derived using the $Z \rightarrow ee$ data and the rejections from the inclusive $W+ \geq 0$ jets sample. The rejections increase slightly as the jet multiplicity in the event increases.

In order to take into account the luminosity dependence of the electron-id efficiency and the probability for finding a track in road (*ie.* PELC finding efficiency), we use exactly the same luminosity for the $Z \rightarrow ee$ sample while

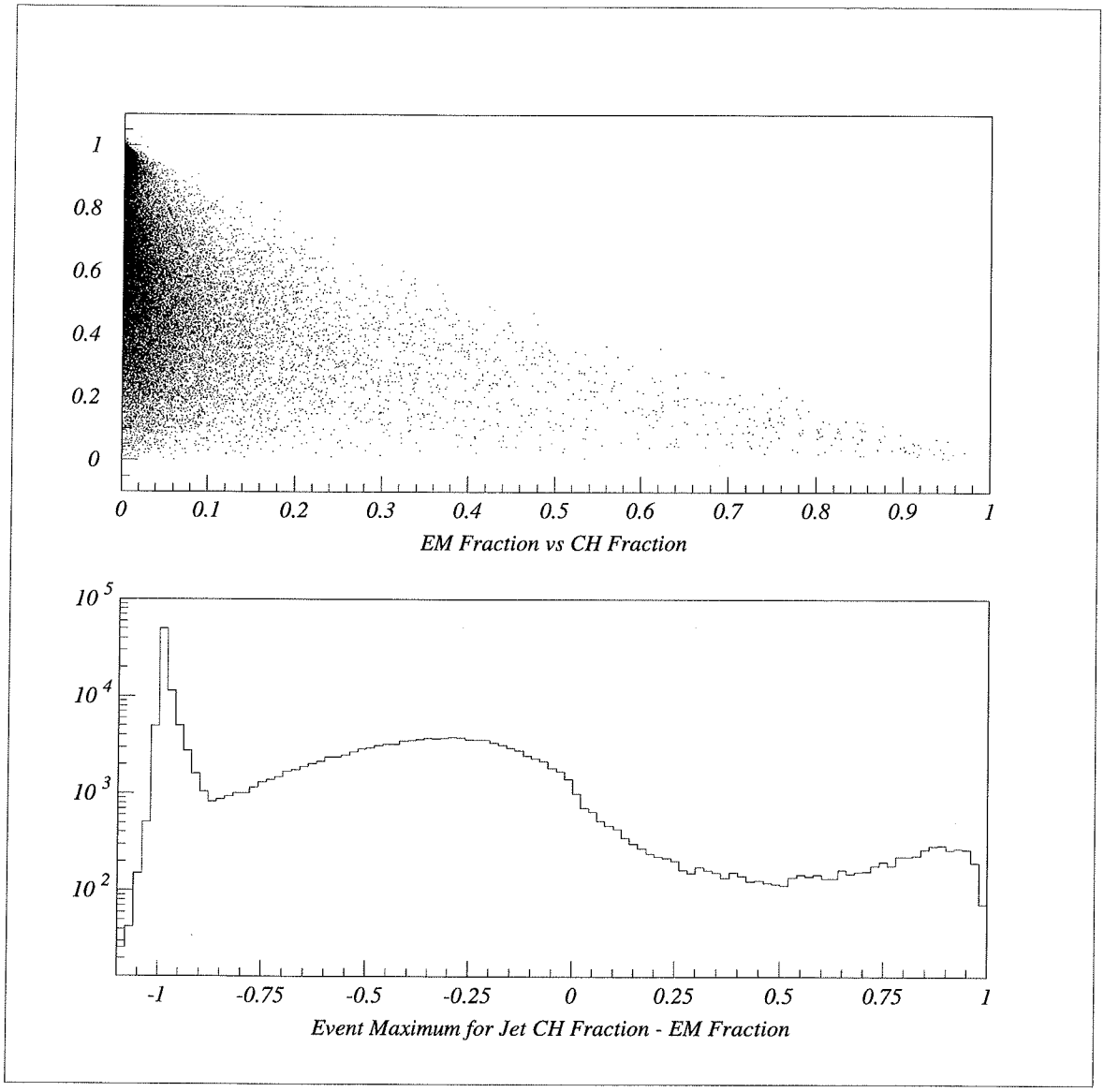

Figure 1: Distribution of CH-fraction vs. em-fraction of jets

Table 2: Comparison of electron-id using 4-var likelihood with "old" electron-id used in top analyses

Efficiency and Rejections		
cut	Efficiency(%)	Rejection
new eid : 4-variable likelihood		
CC (tight)	81.1±1.0	46±1
EC (tight)	51.4±1.8	25±2
old eid : Conventional Cut		
CC (tight)	82.6±1.0	36±1
EC (tight)	50.9±1.5	19±2

deriving the efficiencies as the e+jets sample used in the analysis. All of the efficiencies obtained using the $Z \rightarrow ee$ sample are listed in table 3.

Most of the Monte Carlo samples used by the top analyses are generated using the SHOWERLIBRARY MC. While selecting electrons in these MC samples we require an isolated PELC to match with an ISAJET electron. We do not impose the electron-likelihood cut at the Monte Carlo level. They are propogated from those measured from $Z \rightarrow ee$ events. We also correct the PELC finding efficiencies by the difference between the tracking efficiency observed in $Z \rightarrow ee$ events in data and those generated using SHOWERLIBRARY MC.

5.2 Muon-id

Two types of muon identification are used in this analysis. They correspond to selecting muons arising dominantly from the $W \rightarrow \mu\nu$ decay and from the decay $b \rightarrow \mu + X$. The first class is denoted as *isolated* muons, and the second class is denoted as*tag* muons. The run Ib selection requirements for each type are described separately in the following two sections. The corresponding Ia definitions can be found in reference [4].

Table 3: Electron identification efficiencies used in lepton+jets analyses

Efficiency(%)		
	CC	EC
4-var likelihood(tight) + isolation	81.1±1.0	51.4±1.8
SHLB tracking efficiency (monte carlo)	94.75±0.64	90.69±1.57
Data tracking efficiency ($\geq$ 1 vertex events)	82.67±1.07	85.19±1.02
Data tracking efficiency ($\geq$ 2 vertex events)	77.08±1.59	82.23±1.63
Data tracking efficiency ($\geq$ 3 vertex events)	69.96±4.89	81.56±5.05
Data tracking efficiency (= 1 vertex events)	85.82±1.06	86.97±1.22
Data tracking efficiency (= 2 vertex events)	77.89±1.57	82.32±1.73

Events taken during the MRBS_LOSS gate are used in this analysis after having the calorimeter based quantities corrected for main ring energy. [10] The muon reconstruction efficiency is lower for muons taken during this period because of voltage sag in the muon system. An $\int L \cdot \epsilon$ correction has been determined using events with identically two jets and one high-p_t non-isolated muon (See below). There are 35891 such events occuring passing the GOOD_BEAM requirement, and 3921 events which occur during the MRBS_LOSS veto[1] The overall increase in luminosity times efficiency arising from the MRBS_LOSS data is thus $3921/35891 = 10.9 \pm 0.2\%$.

5.2.1 Isolated Muons

The selection requirments for isolated muons in run Ib data are

- Muon Quadrant $\leq 4 (\leq 12)$ for runs$< 89,000 (\geq 89,000)$
- IFW4$\leq 1(0)$ for CF(EF) muons.
- (HFrac ≥ 0.75 and EFrac_H(1)> 0) or HFrac $= 1.0$
- A-stubs vetoed
- $r_{IP} \equiv \sqrt{IP_{BV}^2 + IP_{NB}^2} \leq 20.0$ cm
- $\int \vec{B} \cdot \vec{dl} \geq 0.6$ GeV
- $p_t \geq 20$ GeV/c
- $\Delta R \geq 0.5$

The first item is a fiducial cut corresponding to $\eta \leq 1.0(1.7)$ for CF(EF). The second item indicates reasonable quality-of-fit of the muon using information from the muon system only. The third item is often referred to as "MTC" [11] and serves both to reject combinatoric fakes and cosmic rays. The fourth item rejects muon tracks having no B/C layer hits. The fifth item provides further protection against cosmic ray muons and misreconstructed muons. Here IP_{BV} and IP_{NB} are the 2D distances-of-closest approach between the muon and the associated vertex in the bend and non-bend projections. The

[1]The MICRO_BLANK period is always explicitly excluded.

Requirement	Efficiency (%) CF	EF
w/good PMUO	$\equiv 1.0$	$\equiv 1.0$
w/good PMUO, $p_t > 20$	89.6 ± 0.5	72 ± 2
remaining ID cuts	80.4 ± 0.7	68 ± 2
ΔR isolation	65.9 ± 0.8	61 ± 2

Table 4: Efficiency for muons from W decay passing the selection requirements. The efficiency is given separately for CF and EF and is normalized to the number of muons passing the IFW4 and MTC requirements. The ΔR efficiency is dependent on the physics signal through the jet-multiplicity dependence. The number quoted is for simulated top events.

$\int \vec{B} \cdot \vec{dl}$ requirement insures that muons have traversed enough field to give an acceptable p_t measurement. The p_t and ΔR requirements select muons characteristic of those from W decay. Here ΔR is the distance in η, ϕ space between the muon and the nearest 0.5 cone jet.

The muon reco efficiency is expressed as the product of three components. The first is the probability that a real muon gives rise to a PMUO bank passing the IFW4 and MTC requirements assuming ideal hit finding efficiencies. The second component is a correction factor accounting for the true hit-reconstruction efficiency. The third component is the efficiency for passing all other requirements.

The uncorrected "PMUO" efficiency is determined using Monte Carlo and is found to be $75 \pm 1\%$ for high-p_t muons in the CF and $85 \pm 1\%$ for high-p_t muons in the EF. The correction factor is determined using μsmeared Monte Carlo and is 90 ± 2(sys)% for untriggered high-p_t muons in the CF and 95% for triggered CF muons. The EF post-zap "PMUO" efficiency correction is 85 ± 2.

The efficiency for the remaining requirements is determined from Monte Carlo. Table 4 shows the efficiencies derived from simulated $t\bar{t}$ events.

5.2.2 Tag Muons

The selection requirments for tag muons in run Ib data are

- Muon Quadrant $\leq 4(12)$ for runs $< 89,000(\geq 89,000)$
- IFW4$\leq 1(0)$ for CF(EF) muons
- (HFrac ≥ 0.75 and EFrac_H(1)> 0) or HFrac $= 1.0$
- A-stubs vetoed
- $p_t \geq 4$ GeV/c
- $\Delta R < 0.5$

The first item is a fiducial cut corresponding to $\eta \leq 1.0(1.7)$ for CF(EF). The second item indicates reasonable quality-of-fit of the muon using information from the muon system only. The third item is often referred to as "MTC" and serves both to reject combinatoric fakes and cosmic rays. The fourth item rejects muon tracks having no B/C layer hits. The p_t and ΔR requirements select muons characteristic of those from heavy flavor decay. Here ΔR is the distance in η, ϕ space between the muon and the nearest 0.5 cone jet.

The muon reconstruction efficiency is expressed as the product of three components. The first is the probability that a muon gives rise to a PMUO bank passing the IFW4 and MTC requirements for ideal hit reconstruction efficiency. The second component is a correction factor accounting for losses introduced by hit-finding ineffiencies. The final piece is the efficiency for passing all other requirements.

The "PMUO" efficiency for muons arising from the decay of heavy quarks is determined using Monte Carlo and ranges from 38% to 55% depending on top mass. The mass dependence arises because the average tag p_T increases with increasing top mass, thereby causing more muons to penetrate the iron of the toroids and pass the 4 GeV p_T threshold. The efficiencies are the same for the CF and EF regions. The hit-finding efficiency-correction factor is found to be 90 ± 2(sys)% for tag muons in the CF, and 84 ± 2% for tag muons in the post-zap EF.

The efficiency for the remaining requirements is determined from both Monte Carlo and data. These results are contained reference [2]. Table 5 shows final the efficiencies and background from this document.

Detector Region	Efficiency(%)	Background(%)
CF	94.7 ± 0.4	3.9 ± 1.9
EF	88.5 ± 3.3	7.9 ± 4.2

Table 5: Tag muon efficiency and background for CF and EF(Run$\geq$89,000) muons.

5.3 Jets and Missing Et

Jets are reconstructed with a fixed cone algorithm. We use a cone size of dR = 0.5. All the jets are corrected with CAFIX V5.0. These jets are required to have a minimum E_t of 15GeV and be within $\mid \eta \mid \leq 2.0$.

Two different definitions of $\not\!\!E_T$ (corrected using CAFIX) is used :

- $\not\!\!E_T^{cal}$: the calorimeter missing E_T, (PNUT4)
- $\not\!\!E_T$: the muon corrected missing E_T, (PNUT5)

In D0RECO we suppress the hot cell in the events using two different algorithms. One of them suppresses the calorimeter cells which were detected to be 'HOT' due to known hardware problems. The other algorithm, AIDA suppresses cells which are 'HOT' due to random discharges in the event. Since AIDA only uses the longitudinal energy deposition pattern to determine if the cell is isolated, it often finds cells in a jet as hot. These falsely suppressed 'HOT' cells in events then give rise to false $\not\!\!E_T$. Therefore we further correct the calorimeter missing E_T (PNUT4) in the event to account for this problem. If a hot cell classified in the CAID bank is within δR of 0.25 of a jet then it is added back vectorially to the calorimeter $\not\!\!E_T$ of the event. In all the analyses in this note we use this corrected definition of $\not\!\!E_T$

6 Triggers

6.1 Electron Triggers and Efficiency

The trigger efficiency for W + jet events has been estimated from the data as a function of jet multiplicity. The present analyses in the Run 1b

e+jet channels use 2 triggers, ELE_JET_HTGH and EM1_EISTRKCC_MS. ELE_JET_HIGH required at level 1, 1 em tower $E_T \geq$12 GeV, $\mid \eta \mid \leq$ 2.6, and an additional jet tower, $E_T \geq$5 GeV, $\mid \eta \mid \leq$ 2.6, and at level 2, an ELE electron, $E_T \geq$ 15 GeV, an additional jet, $E_T \geq$10 GeV and 14 GeV of Missing Transverse Energy. EM1_EISTRKCC_MS required required at level 1, 1 em tower $E_T \geq$12 GeV, and at level 2, an EIS electron with a track, and 15 GeV of Missing Transverse Energy. The additional jet requirement in ELE_JET_HIGH, introduces a jet multiplicity bias in this trigger.

To measure the trigger efficiency of the two trigger and then to do a joint trigger efficiency, we will factor triggers into electron, $\not\!\!E_T$ and jet parts, measure the efficiency of a given part for W events and then combine the results, making the assumption that the trigger efficiency factorizes.

Table 6: ELE_JET_HIGH jet trigger efficiency. Tabulated is the efficiency for ELE_JET_HIGH to trigger on the additional jets in a W + n jets events. Tabulated is the fraction of W events passing EM1_EISTRKCC_MS which also pass ELE_JET_HIGH as a function of jet multiplicity. This is the trigger efficiency for the Level 1 requirement of one jet tower, $E_T \geq$ 5 GeV and the Level 2 requirement of 1 jet, 0.3 cone Jet with $E_T \geq$ 10 GeV. Offline reconstructed jets are required to be within $\mid \eta \mid \leq$2.0 and pass either a 15 or 20 GeV transverse energy cut.

Multiplicity	Eff (E_Tj$\geq$15 GeV)	Eff (E_Tj$\geq$20 GeV)
0	1.6 $\pm$ 0.1%	3.6 $\pm$ 0.1%
1	60.2 $\pm$ 0.6%	77.5 $\pm$ 0.6%
2	84.4 $\pm$ 1.0%	95.1 $\pm$ 0.8%
3	94.8 $\pm$ 1.4%	99.2 $\pm$ 0.8%
4	96.5 $\pm$ 2.4%	100.0 $\pm$ 4.6%

6.1.1 Electron Trigger Efficiency

To measure the electron efficiency, we require a trigger without any electron requirement. We require a W (i.e. a good electron and $\not\!\!E_T$) and then ask if the electron has satistfied the trigger. To get a sample of W's, we start by requiring the MISSING_ET filter with requires 35 or 40 GeV of $\not\!\!E_T$. We

then ask if the electron for the W's found satisfies, the ELE or EISTRKCC requirement of the trigger. We find that the ELE (EISTRKCC) is 98.7 $\pm$ 0.1% (95.6 $\pm$ 0.2%) (statistical error only) efficient for 20 GeV Electron passing top electron id requirements.

6.1.2 $\not\!\!E_T$ Trigger Efficiency

To measure the $\not\!\!E_T$ trigger efficiency, we start with a monitor trigger, require a W, and impose the level 2 $\not\!\!E_T$ requirement. For a level 2 $\not\!\!E_T$ requirement of 15 GeV, we find the efficiency is 99.1 $\pm$ 0.1% (99.6 $\pm$ 0.1%) (statistical error only) for an offline $\not\!\!E_T$ cut of 20 (25) GeV.

6.1.3 Jet Trigger Efficiency

To measure the ELE_JET_HIGH efficiency as a function of jet multiplicity, we require a W passing EM1_EISTRKCC_MS and then observe (as a function of jet multiplicity) how many W events pass ELE_JET_HIGH. The results of this analysis are shown in table 6

6.1.4 Overall Trigger Efficiency

The overall trigger efficiency is shown in table 7. The errors shown are combined statistical and systematic. A flat 3% systematic error has been assumed for the individual trigger efficiencies.

6.2 Muon Triggers and Efficiency

The following triggers were used in the μ+jets analyses:

- MU_JET_xxxx family:
  - MU_JET_HIGH
  - MU_JET_CAL
  - MU_JET_CENT and
  - MU_JET_CENCAL
- JET_3_xxxx family:

Table 7: Electron + Jet Trigger Efficiencies. Shown are the efficiencies for EM1_EISTRKCC_MS & ELE_JET_HIGH and their combination. The efficiency of EM1_EISTRKCC_MS is assumed to be independent of jet multiplicity.

		EFFICIENCY (%)			
		$\not\!\!E_T$ ≥20		$\not\!\!E_T$ ≥25	
#j	Filter	E_Tj≥15	E_Tj≥20	E_Tj≥15	E_Tj≥20
	EM1_EISTRKCC_MS	94.7±2.8	94.7±2.8	95.2±2.9	95.2±2.9
0	ELE_JET_HIGH	1.6±0.2	3.5±0.3	1.6±0.2	3.5±0.3
	COMBINED	94.8±2.8	94.9±2.8	95.3±2.8	95.3±2.8
1	ELE_JET_HIGH	58.9±1.9	75.8±2.4	59.2±1.9	76.2±2.4
	COMBINED	96.6±2.3	97.1±2.5	97.1±2.3	97.6±2.5
2	ELE_JET_HIGH	82.6±2.7	93.1±2.9	83.0±2.7	93.5±2.9
	COMBINED	97.3±2.9	97.7±3.0	97.8±2.9	98.2±3.0
3	ELE_JET_HIGH	92.8±3.1	97.0±3.0	93.2±3.1	97.5±3.0
	COMBINED	97.7±3.4	97.8±3.1	98.1±3.4	98.3±3.1
4	ELE_JET_HIGH	94.4±3.7	97.8±5.5	94.9±3.7	98.3±5.5
	COMBINED	97.7±4.4	97.8±7.0	98.2±4.4	98.3±7.0

- JET_3_MISS_LOW
- JET_3_MU and
- JET_3_L2MU

The MU_JET_xxxx triggers are based on a single high p_t muon and a single jet. Both muon and jet are required at level one and level two. The JET_3_xxxx family is based on jet multiplicity at level 1 and level 2 with $\not\!\!E_{\rm T}{}^{cal}$ and loose muon requirements added at level 2. The trigger efficiency is computed separately for both families and the two efficiencies are then convoluted to determine the overall efficiency.

The series of triggers in each family exist because the initial trigger definitions proved unable to cope with increasing instantaneous luminosity. In all cases, the existing triggers were tightened to reduce rate, and a prescaled version of the original definition was kept to allow monitoring. For runs prior to 83213, only the MU_JET_HIGH and MU_JET_CAL triggers existed. Starting with run 83213, the JET_3_xxxx filters were added. Starting with run 89,000, the muon acceptance was extended to include the EF region and CF-restricted MU_JET_CENT and MU_JET_CAL triggers were added.[2]

In addition to these fiducial changes, the muon identification used in the mu+jets filter also changed. The loosest version (that used at the beginning of the run) had no calorimeter confirmation, allowed muons in either CF or EF and used the MUCTAG algorithm for cosmic rejection. The tightest version of the unprescaled trigger used standard calorimeter confirmation, restricted muons to the CF region and used scintillator+MUCTAG for cosmic ray rejection.

The tightest member of each family was unprescaled for all luminosities. The variation in trigger efficiency for the loosest and tightest members of each family is less than 10% [3].[3] At this time, the overall trigger efficiency is not determined more precisely than this level.

The MU_JET_xxxx triggers are $70\pm7\%$ efficient for W+jet and top events having three or more jets. The inefficiency comes almost exclusively from the level 1 muon requirement. For one- and two-jet events the level one trigger-tower requirement introduces a significant inefficiency. The bias is dependent

[2]The original MU_JET_HIGH and MU_JET_CAL filters allow both CF and EF but were prescaled at the higher luminosities for runs occuring after 89,000.

[3]This statement is true for the MU_JET_xxxx family only if the changed fiducial acceptances are ignored.

Run Range	Integrated Luminosity (pb^{-1})	Trigger Efficiency
<83213	15.1	0.70 ± 0.07
≥83213	60.0	0.90 ± 0.09

Table 8: The total trigger efficiency for three or more jet $t\bar{t} \rightarrow \mu +$ Jets, $t\bar{t} \rightarrow \mu +$Jets$+\mu$(tag) and $W+$jet events satisfying all other analysis requirements. The split into two periods reflects the addition of the JET_3_xxxx filters at run 83213.

on the jet thresholds and is measured where needed using a prescaled muon-only trigger as described below in section 9.0.3.

The efficiency for the JET_3_xxxx triggers is less well known. Monte Carlo studies indicate an efficiency for top and $W+$jet events in excess of 85%. Preliminary data-based studies place a strict lower bound of 70% on the efficiency.[4] In further calculations, the JET_3_xxxx efficiency is taken as 70%. The source of the inefficiency is not fully understood.

The total trigger efficiency given by the Monte Carlo approaches 100% for both top and $W+ \geq 4$ jet events. If one assumes uncorrelated inefficiencies between the two families and uses the measured efficiencies, the total trigger efficiency is $\epsilon_{trig} = 90 \pm 10$ (sys)%.

6.3 Muon Acceptance Corrections and Run Dependence

In addition to the changes to the μ+jets analyses triggers, the muon hit-finding efficiency also changed during the run. Significant inefficiency existed in the EF[5] system for the first portion of run Ib. The chambers were cleaned ("zapped") during a shutdown, and the resulting EF chamber efficiency approached the CF efficiency. The pre-zap luminosity for the μ+jets channels

[4]The limiting behaviour of the JET_3_xxxx turn-on curves derived from the data is not yet understood. The plateau occurs at roughly 70% efficiency instead of the expected 95%. Several biases in the selection could account for this effect, and a cleaner study is underway.

[5]The EF muon system covers roughly $1.0 < |\eta| < 1.7$.

Run Conditions	Run Range	$\int L$ (pb^{-1})	Total Trigger Efficiency	Relative Acceptance
CF only, MU_JET_xxxx only	<83213	15.1	0.7	$\equiv 1.0$
CF only, all triggers	83213 – 89000	29.2	0.9	1.0
CF+EF muons, all triggers	>89000	31	0.9	1.5

Table 9: Trigger efficiency and relative geometrical acceptance for top and W+jets events passing analysis requirements.

is 44 pb^{-1}. The post-zap luminosity is 31 pb^{-1}. As indicated in sections 5.2.1 and 5.2.2, muons in the EF region are explicitly excluded from the analysis for the pre-zap period.

Rather than build a variety of Monte Carlo samples to simulate the changing trigger efficiency and analysis acceptance, only the MU_JET_xxxx trigger efficiency and pure CF acceptance is calculated wherever Monte Carlo is used for normalization. A multiplicative correction is then applied to account for the increased efficiency and geometrical acceptance in the later data. The advantage of this method is that ratios of trigger efficiencies are used and that only the luminsity breakdown is required to derive the correction.

Given the changes in trigger and reconstruction efficiency, run Ib is divided into three periods as shown in table 9. The overall multiplicative correction f is given by a sum of efficiencies for the three periods. The correction factor f is given by

$$f = f_1 + f_2 \times (\epsilon_2/\epsilon_1) + f_3 \times (\epsilon_3/\epsilon_1)$$

Here, ϵ_1, ϵ_2 and ϵ_3 are the trigger efficiency*geometrical acceptance for each of the three periods in table [reft-mjcorr. f_i, i=1,3 is the fractional luminosity for the i-th period. As defined here, this correction can never fall below 1.0 ($f_1 = 1.0$). The maximum allowed value arises when $f_2 = 0, f_3 = 1.0 - f_1$. Using the trigger efficiencies and luminosity ratios above and the 2:1 split into CF:EF exhibited by both top and W+jets, a maximum value of $f_{max} = 1.6$ is derived. For the actual luminosity division, using the efficiencies derived from data,

$$f = 1.5 \pm 0.0\ (stat) \pm 0.3\ (sys).$$

A 20% systematic error is currently assigned to this fraction[6] The largest uncertainty in the correction factor is the EF muon reconstruction efficiency. The above value of 1.5 is based on the assumption that the EF post-zap efficiency is similar to CF. The systematic error of 20% is derived assuming EF efficiency is identically zero.

[6]This is likely to be significantly reduced in the near future.

7 Optimization of Cuts using Random Grid Search

Our goal in this analysis is to measure the top production cross section as accurately as possible. With this goal in mind and the fact that the improvements in $lepton - id$ since the **discovery analysis** significantly reduces the contributions from $fake - lepton$ backgrounds, rendering some of the optimized cuts (*e.g. Aplanarity*) obsolete, we embarked on the re-optimization of "Standard Cuts" used to enhance the top contribution in $W+ \geq$3jet events. Also during the last year, there has been major progress made in defining new variables which distinguish top events from backgrounds[5].

The optimization was carried out by using the Random Grid Search Detailed dicusssion of this technique can be found in various writeups[6]. We use the $t\bar{t}$ sample generated with M_{top}=180 GeV as the sample which provides the threshold values for the variables under investigation as well as the sample to compute the expected signal. For the backgrounds we use the appropriate combinations of W+jets and QCD backgrounds. These backgrounds are derived from data for the e+jets+μtag case, whereas for the e+jets(notag) analysis it is a combination of data (qcd) and MC (W+jets). An integrated luminosity of 77pb^{-1} was assued for the optimization.

We attempt to differentiate between $t\bar{t}$ signal and background using the variables $\mathcal{A}$(W + jets), $\mathcal{A}$(jets), $P_T(W)$, $\not\!\!E_T$, H_T(jets), H_T(all) = H_T(jets) + P_T(W), $h = \frac{E_T(lepton)+\not\!\!E_T}{H_T(jets)+P_T(W)}$, N_{jets}. Results of the grid search using these variables or a combination thereof are shown in figures 2 through 5, where the expected number of signal events versus the expected backgrounds are plotted for each threshold value for the variable combination under consideration. A clear boudary that maximizes the expected signal for a given background level is visible and is termed as the 'optimal boundary'. The upper edge of the 'optimal boundary' defines a family of threshold values for various values of signal to background seperation. By comparing these optimal boundary contuors for various combinations of variables, we find that the variables $\mathcal{A}$(W + jets) and H_T(jets) give the best Signal to Noise ratio for a given signal efficiency.

After having chosen the best two parameters for differentiating the top signal, we now have to choose the threshold value for them from the collection of values which lie on the optimal boundary. This is achieved by comparing

the optimal boundary curve to a set of contours which give us constant error in the top production cross section, with the goal of minimizing the error on the cross section measurement as well as contours of constant expected statistical significance. For the smallest acheivable error we choose the threshold value which gives us the best expected statistical significance of the signal.

From figure 2 we find the following cuts ("New Standard" = NS) optimize the Signal to background while keeping the cross section error small in the $lepton + jets$ $(notag)$ channels :

- $\mathrm{H_T(jets)} \geq 180\mathrm{GeV}$
- $\mathcal{A}(\mathrm{W} + \mathrm{jets}) \geq 0.065$

In addition in this channel to further rduce the QCD background we require that

$$\mathrm{E_T^W} = (\not\!\!E_T + \mathrm{E_t(lepton)}) \geq 60\mathrm{GeV}$$

For $lepton + jets$ (μtag) channel, from figure 6, we find the NS cuts to be

- $\mathrm{H_T(jets)} \geq 110\mathrm{GeV}$
- $\mathcal{A}(\mathrm{W} + \mathrm{jets}) \geq 0.04$

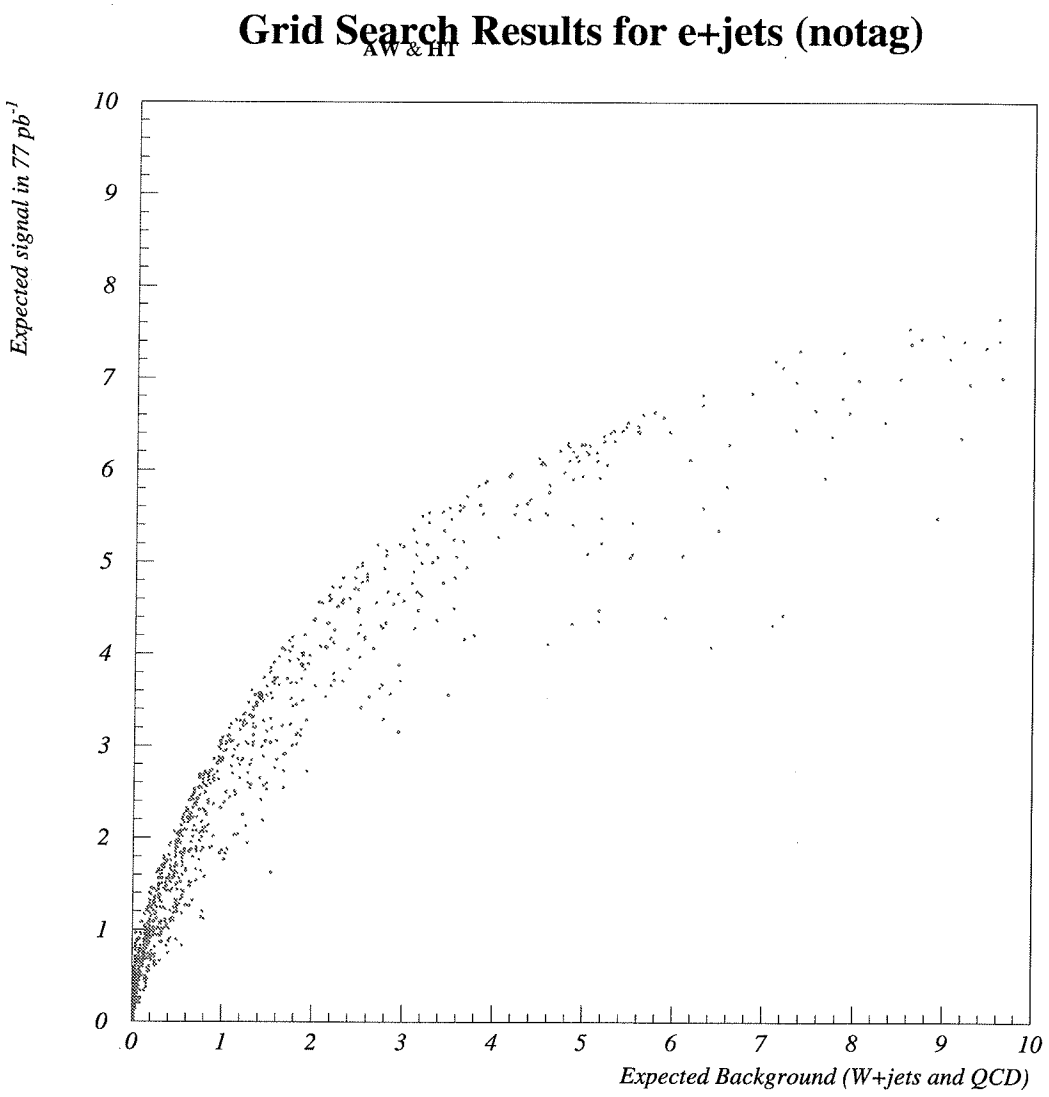

Figure 2: Grid Search results for $e + jets$ channel using variables $\mathrm{H_T}$(jets) and $\mathcal{A}(\mathrm{W} + \mathrm{jets})$

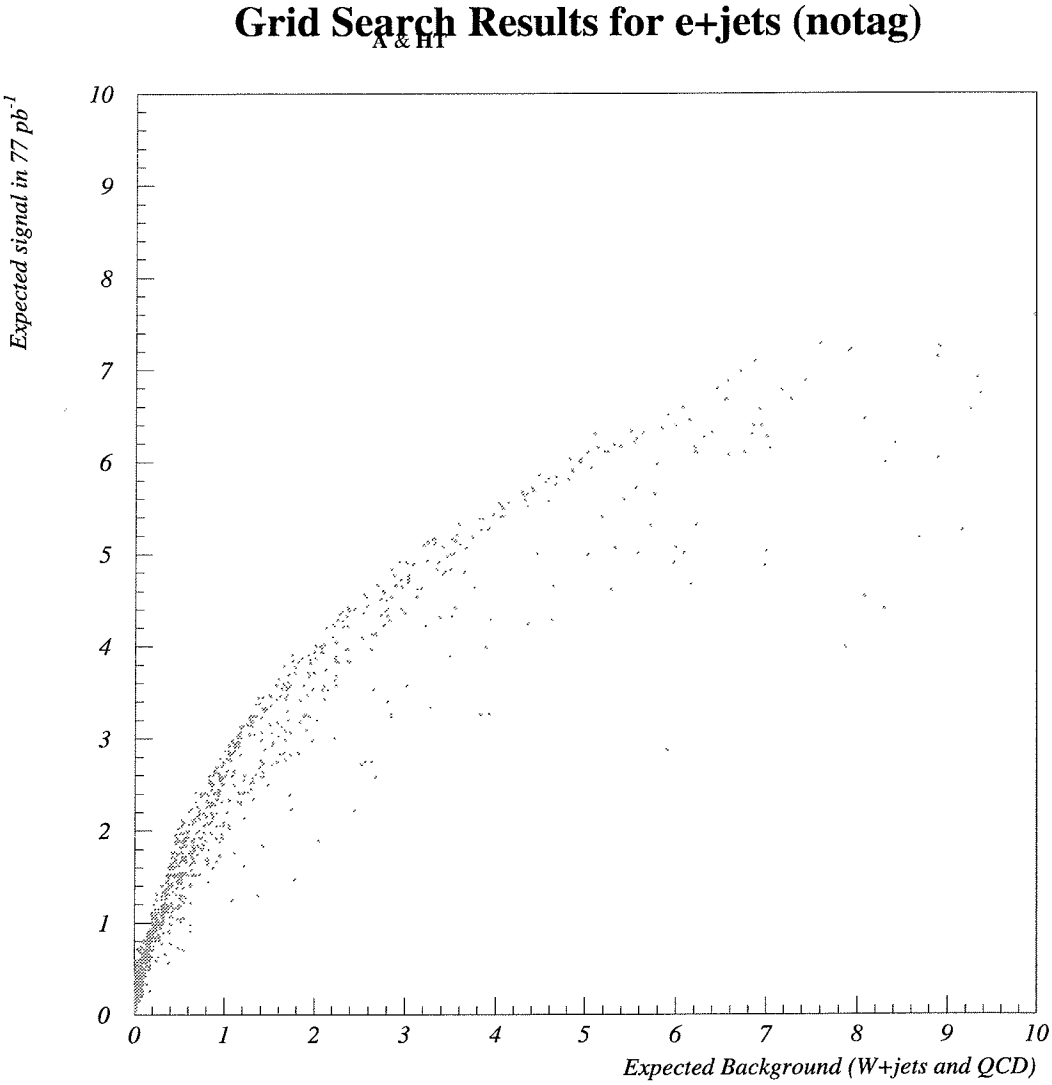

Figure 3: Grid Search results for $e + jets$ channel using variables $H_T(jets)$ and $\mathcal{A}$

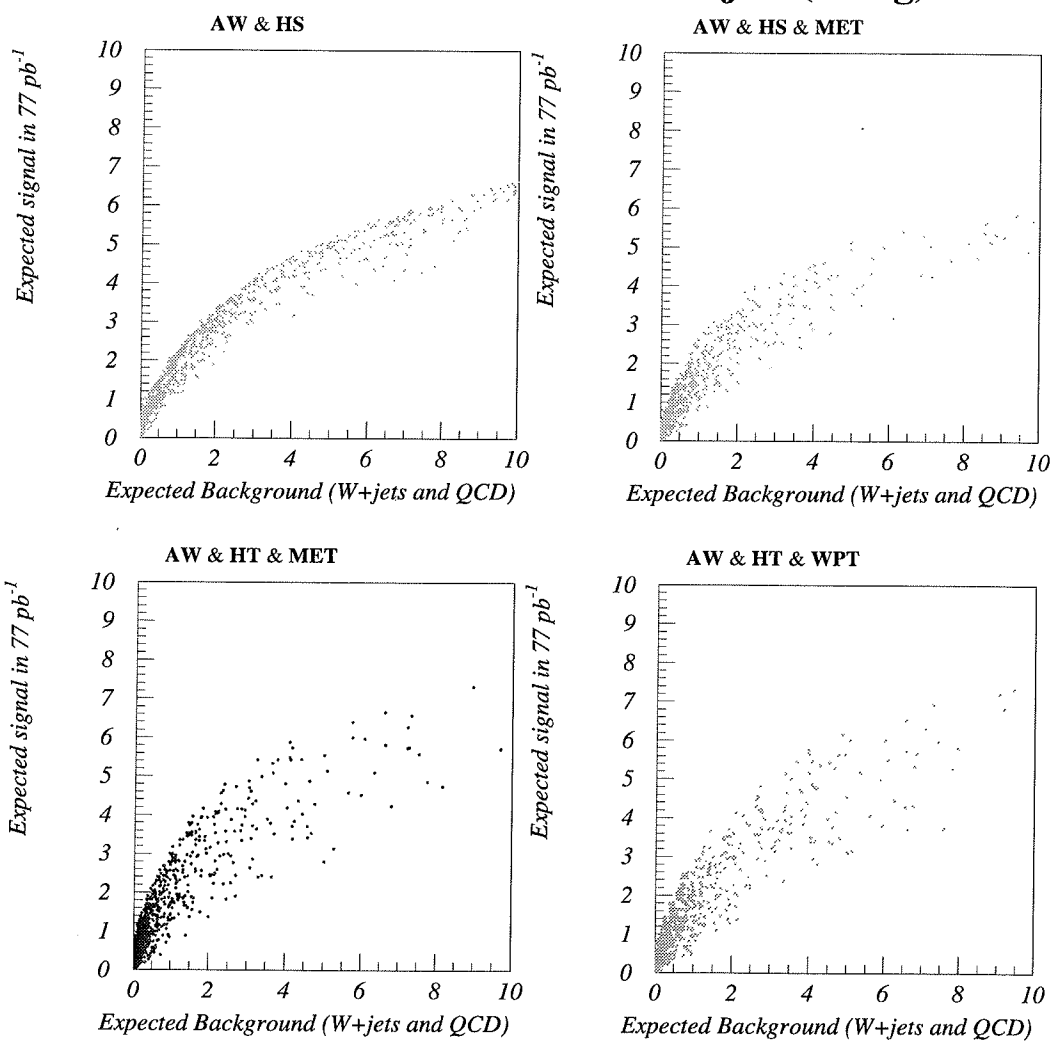

Figure 4: Grid Search results for $e + jets$ channel

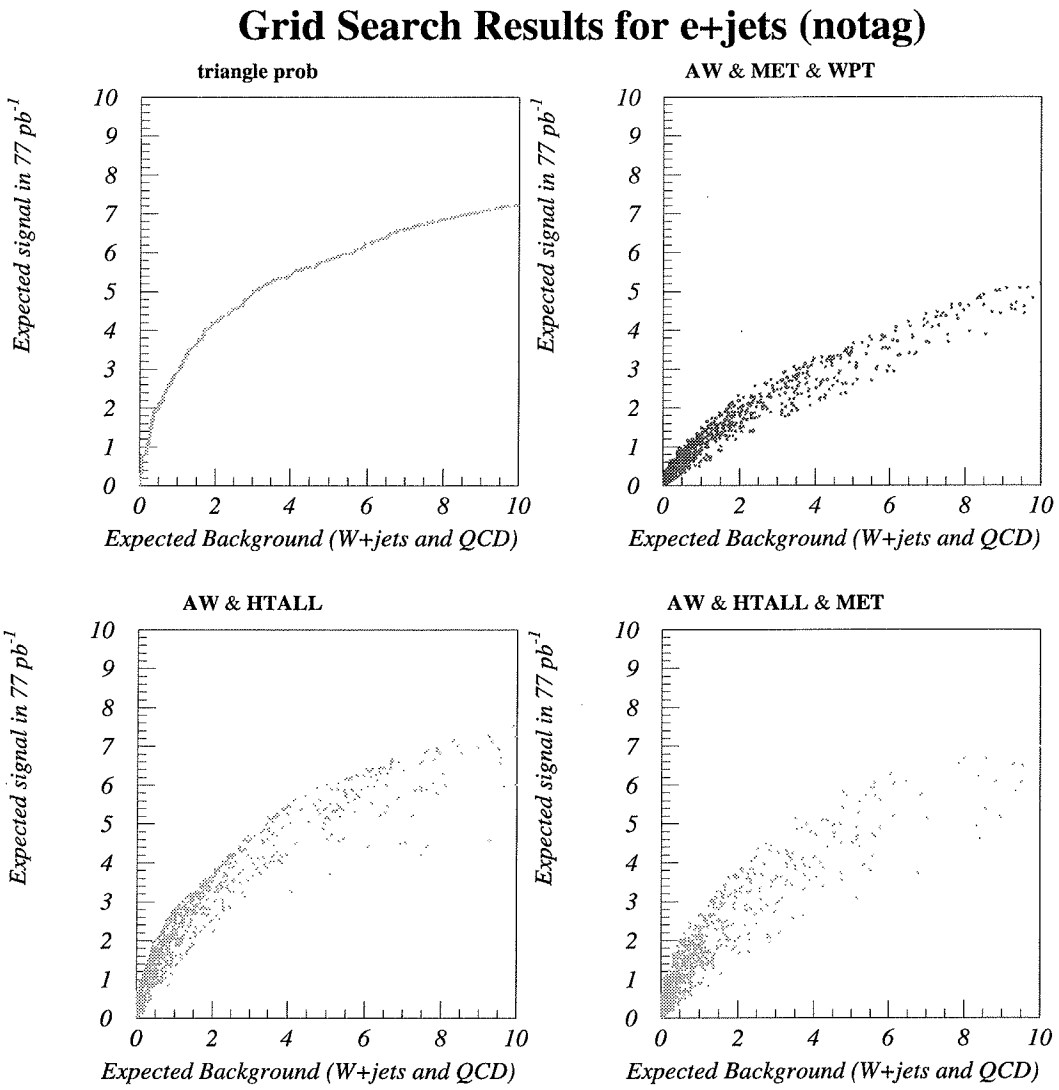

Figure 5: Grid Search results for $e + jets$ channel

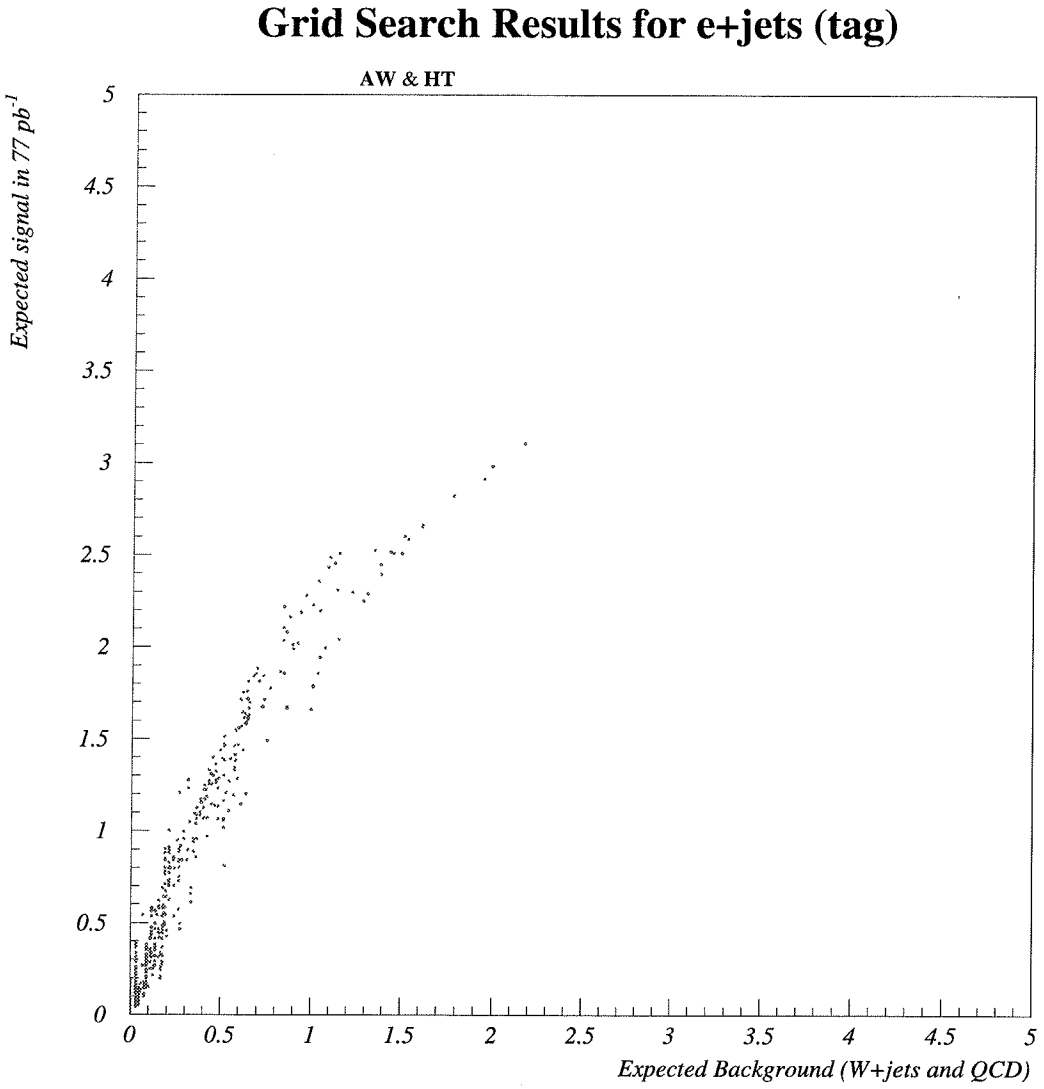

Figure 6: Grid Search results for $e + jets(\mu tag)$ channel using variables $H_T(jets)$ and $\mathcal{A}$

8 Electron+jets (no μ-tag) Analysis

8.1 triggers

The triggers used in this analysis are listed in table 10. The efficiency for the combination is 99.7±0.5% as derived in section 6.1.4.

Table 10: Triggers Used

Run1A	Run1B
ELE_HIGH	ELE_JET_HIGH
ELE_JET	EM1_EISTRKCC_MS

8.2 e+jets event Selection

After the trigger and event cleanup requirements, we select events which satisfy the following requirements :

- one tight electron with $E_t \geq 20$GeV
- $|\eta(\text{electron})| \leq 2.0$
- veto events with on soft muon tags
- $\not\!\!E_T^{cal} \geq 25$GeV
- 1 or more jets with $E_t \geq 15$GeV
- $|\eta(\text{jets})| \leq 2.0$

In tables 11 through 13 the jet multiplicty spectrum of these events is shown for combined Run1A+Run1B sample, Run1B and Run1A samples seperately This base sample is used to obtain the W+jets background in events with at least four jets via Berend's scaling. Detailes will be provided later in the section 8.5.

For the final signal analysis in this channel, we demand the presence of at least four jets with $E_t \geq 15$GeV and $|\eta| \leq 2.0$. At this stage of selection, we find 45 events in Run1B and 10 events in Run1A.

In order to increase signal contribution and reduce the background further in this sample we use the event topology variables $\mathcal{A}(\mathrm{W}+\mathrm{jets})$, $\mathrm{H_T}$(jets) and $\mathrm{E_T^W}$. The cut values are listed below.

- $\mathrm{E_T^W} = (\not\!\!E_T + \mathrm{E_t(lepton)}) \geq 60\mathrm{GeV}$
- $\mathrm{H_T(jets)} \geq 180\mathrm{GeV}$
- $\mathcal{A}(\mathrm{W}+\mathrm{jets}) \geq 0.065$

After the above cuts, we observe 6 events in Run1B and 2 events in Run1A. If we include events in the Main Ring gates, 2 more events pass the above cuts (one each during MRBS_LOSS gate and MICRO_BLANK).

Distributions in $\mathcal{A}(\mathrm{W}+\mathrm{jets})$ vs. H_T for Data, W+4jets, top (M_t = 180 GeV) and QCD background are shown in figure 7. This plot is after the cut on $E_T(W)$.

A run/event list for events in the Base-sample with at least four jets is given below. The events passing the Base-sample and "NS" cuts are indicated by the marker **X**. We also list the $\not\!\!E_T^{cal}$, $\mathcal{A}(\mathrm{W}+\mathrm{jets})$ and $\mathrm{H_T(jets)}$ of these events. In this list the eighth column denotes the events which pass the Ultra-loose sample. The Ultra-loose sample is a super set of the Base-sample, the only difference being that it contains all events with at least 4 jets within $|\eta(\mathrm{jets})| \leq 2.5$.

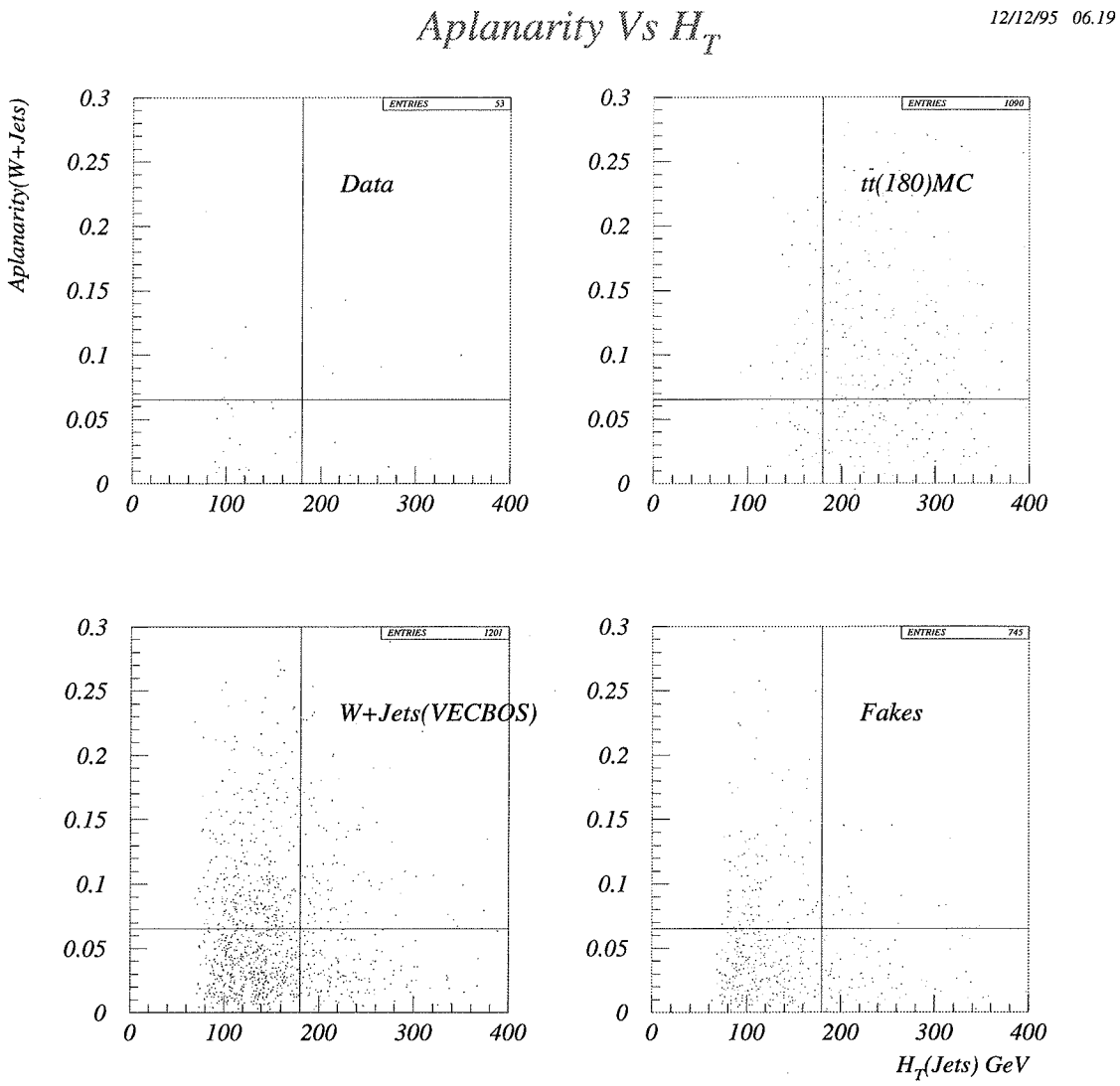

Figure 7: Distributions in $\mathcal{A}$(W + jets) vs. H_T for Data, W+4jets, top ($M_t = 180$ GeV) and QCD background for $e + jets$ analysis

e+jets Run and Event List from Run1A								
Run	Event	$\not\!\!E_T^{cal}$	$\mathcal{A}$(W + jets)	H_T(jets)	Base sample	NS	Ultra-loose	MR gate
54703	9114	27.345	0.033	147.969	X		X	
58381	5028	32.362	0.016	88.615	X		X	
58766	23	25.502	0.010	113.130			X	
61608	9359	30.502	0.010	152.861			X	
61668	7799	39.923	0.010	124.727			X	
62159	2798	35.253	0.017	174.704	X		X	
62199	15224	81.848	0.013	270.551	X		X	
62303	905	28.683	0.010	104.242			X	
62431	788	31.927	0.093	202.051	X	X	X	
62793	920	27.370	0.010	62.771			X	
63066	13373	56.600	0.144	226.721	X	X	X	
64464	21611	79.783	0.058	105.339	X		X	
65288	24705	28.585	0.067	113.996	X		X	
Total					8	2	13	

events during Main Ring activity								
Run	Event	$\not\!\!E_T^{cal}$	$\mathcal{A}$(W + jets)	H_T(jets)	Base sample	NS	Ultra-loose	MR veto
82985	10584	38.487	0.119	200.980	X	X	X	MB
82996	24461	88.587	0.163	170.322	X		X	MRBS
86255	9525	35.082	0.010	88.795			X	MRBS
87063	39091	92.877	0.085	189.519	X	X	X	MRBS
88321	4597	31.884	0.038	268.949	X		X	MRBS
90468	17922	36.871	0.100	177.735	X		X	MRBS
90544	4354	56.072	0.010	133.811			X	MB
92670	18843	42.391	0.010	95.692			X	MRBS
92746	39292	32.647	0.005	101.671	X		X	MRBS
84537	37655	26.014	0.065	110.324	X		X	MB MRBS
88060	14635	33.297	0.004	223.451	X		X	MRBS
91959	5350	48.239	0.037	89.773	X		X	MB
Total					9	2	12	

e+jets Run and Event List from Run1B								
Run	Event	$\not\!\!E_T^{cal}$	$\mathcal{A}$(W + jets)	H_T(jets)	Base sample	NS	Ultra-loose	MR veto
76143	14180	25.658	0.011	114.711	X		X	
80932	41	54.277	0.010	260.591			X	
81543	21845	42.982	0.013	93.869	X		X	
81949	12380	36.583	0.040	172.557	X		X	
82024	44002	49.895	0.008	91.990	X		X	
82220	20012	32.217	0.032	112.880	X		X	
82254	30713	29.882	0.005	140.521	X		X	
82343	28594	82.375	0.010	66.525			X	
83040	2635	28.902	0.010	72.580			X	
84331	13271	30.264	0.108	87.413	X		X	
84890	28925	47.686	0.026	96.602	X		X	
85287	16834	60.334	0.010	141.727			X	
85439	40481	47.554	0.010	51.587			X	
85689	24599	72.568	0.007	228.344	X		X	
85782	2046	26.550	0.010	105.002			X	
85917	22	54.582	0.027	395.691	X		X	
86211	14712	40.027	0.073	118.830	X		X	
86214	17756	27.860	0.033	103.430	X		X	
86217	10075	31.049	0.011	125.907	X		X	
86518	11716	89.392	0.064	285.286	X		X	
86601	33128	33.044	0.086	215.863	X	X	X	
87070	30533	38.021	0.101	346.467	X	X	X	
87104	25823	26.875	0.027	179.435	X		X	
87329	13717	27.833	0.091	260.692	X	X	X	
87446	14294	53.686	0.098	99.779	X		X	
87448	15723	41.789	0.010	77.476			X	
87910	10959	28.904	0.010	96.210			X	
88018	29752	35.889	0.010	61.149			X	
88038	14829	36.325	0.210	79.377	X		X	
88044	9807	46.403	0.033	165.652	X		X	
88045	35311	95.529	0.135	189.952	X	X	X	
88125	15437	48.765	0.123	123.929	X		X	
88463	3627	30.307	0.048	91.120	X		X	
88532	33633	43.117	0.010	85.818			X	

e+jets Run and Event List from Run1B (cont'd)								
Run	Event	$\not\!\!E_T^{cal}$	$\mathcal{A}$(W + jets)	H_T(jets)	Base sample	NS	Ultra-loose	MR gate
88588	15993	39.167	0.068	99.056	X		X	
88600	864	34.217	0.010	56.670			X	
89484	11741	34.866	0.065	146.011	X		X	
89550	18042	36.290	0.064	92.250	X		X	
89708	24871	92.620	0.075	177.718	X		X	
89815	17253	60.733	0.097	202.490	X	X	X	
89936	6306	59.109	0.033	215.294	X		X	
89972	13657	42.467	0.086	177.588	X		X	
90108	31611	35.847	0.035	165.298	X		X	
90435	32258	69.148	0.065	131.525	X		X	
90439	12802	34.840	0.010	54.074			X	
90455	1247	60.556	0.010	264.127			X	
90496	28296	31.967	0.071	115.028	X		X	
90693	8678	25.693	0.152	66.143	X		X	
90795	14246	32.246	0.023	155.059	X		X	
90804	6474	54.428	0.052	106.275	X		X	
91855	23647	28.699	0.019	312.589	X		X	
91923	502	71.801	0.059	150.441	X		X	
92013	11825	28.887	0.033	127.946	X		X	
92081	4086	54.997	0.002	125.809	X		X	
92143	28632	104.778	0.010	159.929			X	
92217	109	45.416	0.280	103.600	X		X	
92278	21744	50.633	0.005	118.386	X		X	
92673	4679	38.641	0.109	422.136	X	X	X	
92673	30298	27.525	0.062	102.279	X		X	
Total					45	6	59	

8.3 Distributions of e+jets events

$\mathcal{A}$(W + jets) ↓	H_T(jets) < 180	H_T(jets) ≥ 180	H_T(jets) < 180	H_T(jets) ≥ 180	H_T(jets) < 180	H_T(jets) ≥ 180	H_T(jets) < 180	H_T(jets) ≥ 180
< 0.065	21	5	610	198	385	109	101	367
≥ 0.065	13	6	395	124	215	41	110	680
	Data Run1B		W+**4j(VB)**		**QCD Run1B**		$t\bar{t}$ (180) GeV	
< 0.065	4	1			34	15		
≥ 0.065	1	2			12	5		
	Data Run1A				**QCD Run1A**			

After $E_T(W)$ cut

$\mathcal{A}$(W + jets) ↓	H_T(jets) < 180	H_T(jets) ≥ 180	H_T(jets) < 180	H_T(jets) ≥ 180	H_T(jets) < 180	H_T(jets) ≥ 180	H_T(jets) < 180	H_T(jets) ≥ 180
< 0.065	21	5	593	194	223	71	95	361
≥ 0.065	13	6	380	120	102	18	108	663
	Data Run1B		W+**4j(VB)**		**QCD Run1B**		$t\bar{t}$ (180) GeV	
< 0.065	4	1			21	13		
≥ 0.065	0	2			8	5		
	Data Run1A				**QCD Run1A**			

8.4 Comparison of Inclusive Jet Multiplicity Spectra

In figure 12 we plot the inclusive jet multiplicity distribution observed in Run1B as a function of two minimum jet E_T cut off at 15 GeV and 25 GeV. For guiding the eye we draw a straight line through the first two multiplicity points for each jet E_T threshold. Even at this stage of analysis, where we are swamped by $W + jets$ backgrounds, we can observe a slight excess of events with at least 4 jets.

In this plot one can clearly notice a feature of the data, *ie.* the exponential decrease of the number of events as a function of jet multiplicity. This is also expected from Theoretical predictions.[9] This behaviour is also seen in Monte Carlo eneration of $W +$ jets events. [9] Figure 13 shows the inclusive jet multiplicity distribution both for our data sample and the predictions of the VECBOS MC as function of three different jet E_T thresholds. VECBOS predictions are computed using the cross sections obtained from MC itself. From this figure we conclude that the agreement between our observation and the MC predictions are very good.

8.5 Backgrounds

There are two sources of major backgrounds in this channel

A. non-W background (also known as QCD or $fake - electron$ background)

B. $W(\rightarrow e\nu) +$ jets

For estimating the non-W background (or QCD background) for a given jet multiplicity we use three different methods :

1. $\not\!\!E_T$ scaling method (QCD fraction)
2. four quadrant fit to electron quality and $\not\!\!E_T^{cal}$
3. Ratio of good to bad electrons in the signal region

Detailed description of these methods can be found in various notes.[8] The contribution from QCD background to various jet multiplicity for all samples are listed in the third column of tables 11 – 13.

Table 11: Inclusive Jet multiplicty for e+jets events (Run1A and Run1B)

Run1A & 1B data, $\int \mathcal{L}dt = 90.9\text{pb}^{-1}$			
minimum no. of jets	#of events	# QCD bkg	Total - QCD (N^{obs})
1	9014	287.54±16.69	8726.46±105.62
2	1620	238.29±14.25	1381.71± 46.13
3	298	60.57± 6.95	237.43± 18.58
4	55	12.53± 3.11	42.47± 8.06

We fit the number of W's (see table) for different jet multiplicities, to the equation

$$N_i^{obs} = N_1^W * \alpha^{(i-1)} + f_i * N^{top}$$

Where,

N_i^{obs} : # of events observed at Jet Multiplicity 'i' after removing contribution from non-W backgrounds (last column of tables 11 – 13).

f_i : Fraction of $t\bar{t}$ events expected at multiplicity 'i'

α : ratio of multiplicities

N_1^W : Number of W+1jet events

N^{top} : Number of top events in our sample

The last three variables are results of the fit. These are listed in table 14 for the different data samples. The QCD background subtracted inclusive jet multiplicity spectra for run1A and Run1B with the fit superposed are shown in figures 14 and 15.

From these fits, we compute the contribution in the base e+4jets from W+4jets background and its error using the following equations :

Table 12: Inclusive Jet multiplicty for e+jets events in Run1A

Run1A data, $\int \mathcal{L}dt = 13.6\text{pb}^{-1}$			
minimum no. of jets	#of events	# QCD bkg	Total - QCD (N^{obs})
1	1675	53.43± 5.03	1621.57± 57.56
2	296	40.22± 3.32	255.78± 24.39
3	54	11.16± 1.11	43.84± 7.22
4	10	2.28± 0.61	7.72± 3.19

$$N_4^W = N_1^W * \alpha^3$$

$$\delta N_4^W = N_4^W * \sqrt{\left(\frac{\delta N_1^W}{N_1^W}\right)^2 + 3 * \left(\frac{\delta\alpha}{\alpha}\right)^2}$$

Finally, the component for each species of background in the NS sample is derived by folding the "NS" cut survival probability of these backgrounds to the contribution from each of them to the base e+4jets sample.

$$N_{total}^{bkg} = N^{QCD} * f_{QCD} + N^W * f_W$$

where,

N^{QCD} = N*(amount of QCD) from table

N^W = $N - N^{QCD}$

f_W = "NS" cut survival probability for Vecbos W+4jet sample

= 0.091

f_{QCD} = "NS" cut survival probability for $fake-electron$+4jets sample.

= 0.025

Table 13: Inclusive Jet multiplicty for e+jets events in Run1B

Run1B data, $\int \mathcal{L}dt = 77.3\text{pb}^{-1}$			
minimum no. of jets	#of events	# QCD bkg	Total - QCD (N^{obs})
1	7339	234.11±22.19	7104.89± 88.49
2	1324	198.07±14.44	1125.93± 39.15
3	244	50.41± 7.01	193.59± 17.12
4	45	10.25± 3.11	34.75± 7.40

Table 14: Results of the Berends fit to e+jets data sample

Data Sample	α	N_1^W	N^{top}
Run1A	0.159 ± 0.02	1611.2±151.55	2.8± 8.4
Run1B	0.162 ± 0.007	7088.2±88.26	15.1±16.8

The final background estimations are summarized in table 15. Wherever there are two errors quoted in table 15, the first is statistical and the second is systematic. The systematic error analysis is described in the next section.

8.6 Systematic Error sources in Background determination

The major sources of systematic errors in the estimate of the backgrounds to the e+jets channel are :

- Berend's scaling(i.e. how well the data follows this rule)
- Jet energy Scale
- Difference in H_T distribution for data and VB

Table 15: Estimated backgrounds in ejets sample before and after "NS" cuts

	Base sample			"NS" sample		
Run	W+4jets	QCD	total	W+4jets	QCD	total
1A	6.20±4.49	2.28±0.65	8.5±4.5	0.56±0.41±0.10	0.06±0.02	0.6±0.4±0.1
1B	26.62±11.0	10.25±3.11	36.5±11.4	2.40±0.99±0.45	0.25±0.10	2.7±1.0±0.5

Table 16: Estimated backgrounds in ejets sample after "NS" cuts scaled to MAX_LIVE luminsoity

	"NS" sample		
Run	W+4jets	QCD	total
1A	0.60±0.44±0.11	0.06±0.02	0.66±0.44±0.11
1B	2.83±1.17±0.53	0.30±0.12	3.13±1.18±0.53

8.6.1 Berend's Scaling

We examine variety of data sets(W+jets, QCD multijet, Z+jets and VECBOS W+jets), to estimate this error. We see how well we can predict the number of events with $\geq N$ jets by using the number of events with minimum jet multiplicity $N-1$ and $N-2$.

$$Events(N) = [Events(N-1)]^2/[Events(N-2)]$$

for W+jets Events :

From table 17, the difference in observed and Predicted number of W's is :

- for ≥ 3 jets $[193.59 - (176.16 + 12.36)]/193.59 = 0.026$

Table 17: Data W+jets Events

Jet Mult.	Observed # of W's	Predicted # of W's (From fit to Berends Scaling)	# of TOPs
≥ 1	7104.89±88.49	7088.17±94.16	15.06
≥ 2	1125.93±39.15	1117.44±72.42	14.58
≥ 3	193.59±17.12	176.16±15.98	12.36
≥ 4	34.75± 7.40	27.22± 3.07	8.06

- for ≥ 4 jets $[34.75 - (27.22 + 8.06)]/34.75 = 0.031$

The maximum difference here for ≥ 4 jets is 3.1%.

QCD Fakes :

The QCD fakes are selected as events with a fake electron and $\not\!\!E_T > 25$ GeV. The number of events observed at jet multiplicity are then corrected for the probability of jet to fake as an electron. To obtain this correction factor we count the the number of jets with $E_t > 20$Gev are counted.

Correction Factor = [# of jets with $E_t > 20$GeV]/[# of Events observed]

This factor is normalized to make it 1 for ≥ 1 jet events.

Table 18: QCD Fakes

jet Mult.	# of Events Observed	Correction Factor	Corrected # of Events	Predicted # of events
≥ 1	21566	1.0	21566.0	
≥ 2	8925	1.6	5578.1	
≥ 3	2796	1.9	1471.6	1442.8
≥ 4	774	2.2	351.8	388.2

From table 18, we note that maximum difference between the corrected and predicted number of events is $< 10\%$.

Z+jets Events:

Table 19: Z+jets Data

jet Mult.	# of Events Observed	# of Events Predicted
≥ 0	1697	
≥ 1	265	
≥ 2	40	41.4

Here the difference in observed and predicted # of evtents is $< 4\%$.

VECBOS W+jets :

Table 20 shows # of events/pb^{-1}. We these numbers to verify the Berend's scaling predictions.

Table 20: VECBOS W+jets events/pb^{-1}

jet Mult.	# of Events/pb^{-1}	Predicted # of events
≥ 2	11.6	
≥ 3	2.4	
≥ 4	0.5	0.5

Table 20 show that VECBOS sample follows Berend's scaling to better than 1%.

In addition to these data sets we also looked at the Photon+jets sample and there also the prediction of Berend's scaling hold to better than 5%.

In all the above data sets, the QCD fakes shows maximum difference between observed and predicted values, and we assign 10% Berend's scaling systematic error to our W-Bkg.

8.6.2 Jet Energy Scale

The jet energy scale can effect the e+jets analysis in two ways : first, it can effect the fraction of $t\bar{t}$ events at jet multiplicity and second, it can effect the fraction of VECBOS W+jets events passing the $A - H_T$ cut.

To estimate this uncertainity, we apply the CAFIX nominal, Hi(1 sigma above nominal) and Low(1 sigma below nominal) corrections to our monte carlo sample. Table 21 shows the ratio of 3 to 4 jets events for $t\bar{t}$ montecarlo and table 22 change the fraction if events passing the $A - H_t$ cut for the VECBOS W+jets sample. For this study we have used only $t\bar{t}$(180GeV) sample and VB W+4jet sample.

For $t\bar{t}(180GeV)$:

Table 21: Effect of Energy Scale on $t\bar{t}$ acceptance

jet Mult.	# of Events after CAFIX corrections LOW	Nominal	Hi
≥ 3	1626	1639	1648
≥ 4	1078	1090	1108
N3/N4	0.66	0.67	0.67
# of Evts passing all Cuts	567	582	595

Thus change in N3/N4 is $< 1\%$, and change in acceptance is $< 5\%$.

For VECBOS W+4jets:

Table 22: Effect of Energy scale on fraction of events passing $A - H_t$ cut for VECBOS

	Low	Nominal	Hi
Fraction of Events passing A-H_T cut	0.092	0.093	0.096

Maximum change(table 22) in the fraction of events passing $A - H_t$ cut is 4.3%.

Thus we assign 5% systematic error to W-bkg for jet energy scale.

Table 23: Percent difference in the fraction of events passing the H_T/jet between data and predicted bkg

Jet multi.	% difference
$\geq$2 jets	6%
$\geq$3 jets	10%
$\geq$4 jets (Extrapolated using 2 and 3 jet points)	15%

8.6.3 H_t Difference between data and VECBOS

To determine the systematic error due to difference in the H_T shapes distribution for data and VECBOS, we compare the H_T/jet distribution for the $\geq$2 and $\geq$3 jets events for data and VECBOS, after adding the contributions from TOP and QCD to the VECBOS sample in the appropriate proportion. We also looked at the means of H_T distribution for these data sets. To look at the difference in the distributions, we pick a point on H_T/jet plot which give same Signal/Bkg ratio as the H_T Cut(180GeV). This point is around H_T/jet = 44GeV. (See figures 8- 11).

The differences that we observe between data and monte carlo predicted shapes for H_T/jet cut of 4 GeV are listed in table 23.

Thus we assign an error of 15% to the W Bkg for difference in H_T distribution.

8.7 Top yields and Acceptance

We have used events generated using ISAJET to compute the expected yields from top decays to e+jets. These event samples were generated to include all the possible decay modes for $t\bar{t}$. These are then processed through SHOWERLIBRARY simulation of the DØ detector and reconstructed using DØ RECO V12.20. We then analyze these events (N_{tot}) in exactly the same way as the data to obtain the number of events which pass all the cuts (N_{pass}). The $\epsilon * BR$ thus obtained for this analysis are listed in table 24, which includes a correction for difference in electron-id efficiencies between the SHOWERLIBRARY MC and data derived efficiencies using collider $Z \rightarrow ee$ events and

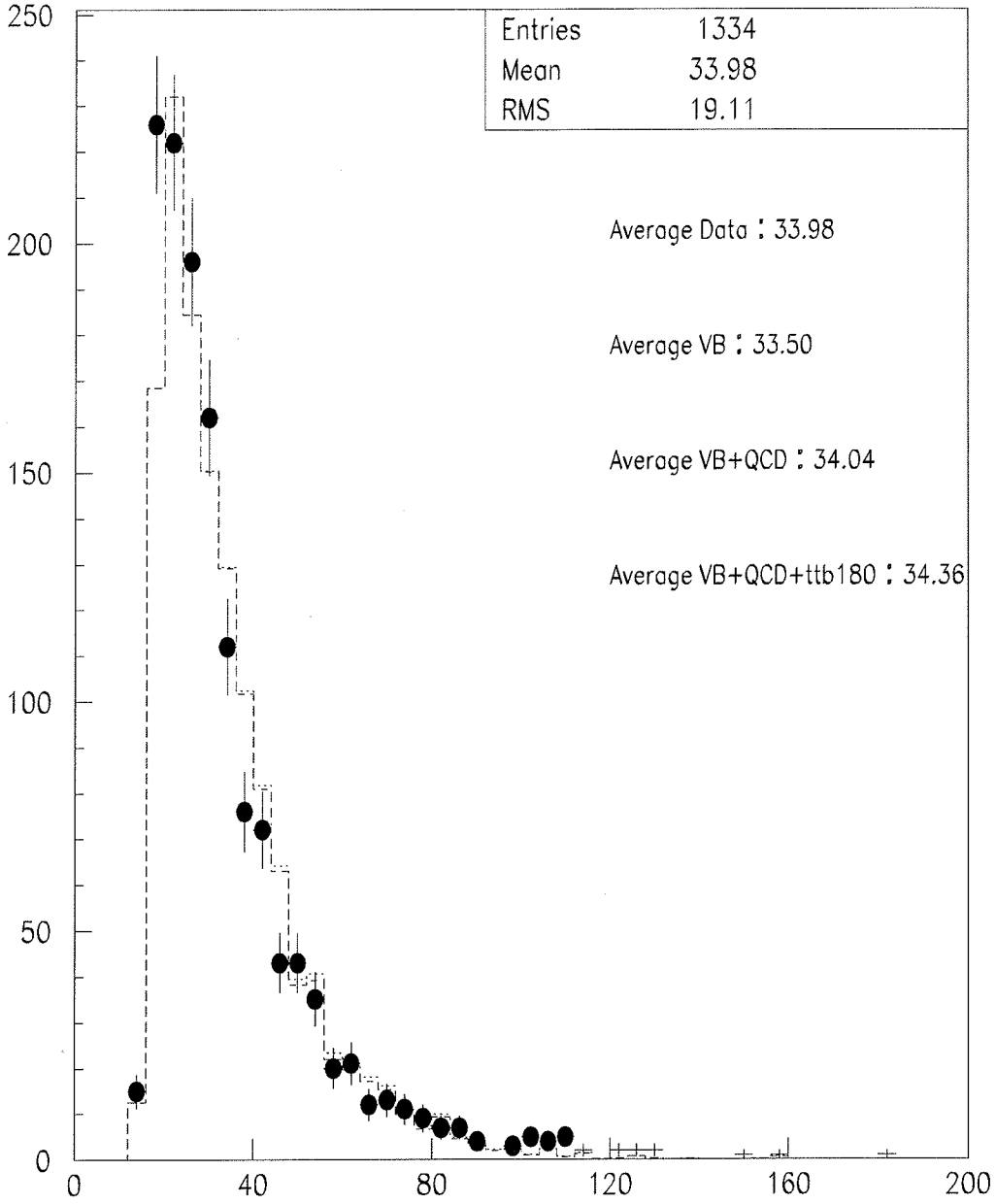

Figure 8: Comparison of H_T/jet distribution for Data and Monte Carlo, for $\geq$ 2jets. Solid histogram is data, dashed is VECBOS+QCD fakes and dotted is VECBOS+QCD+TOP.

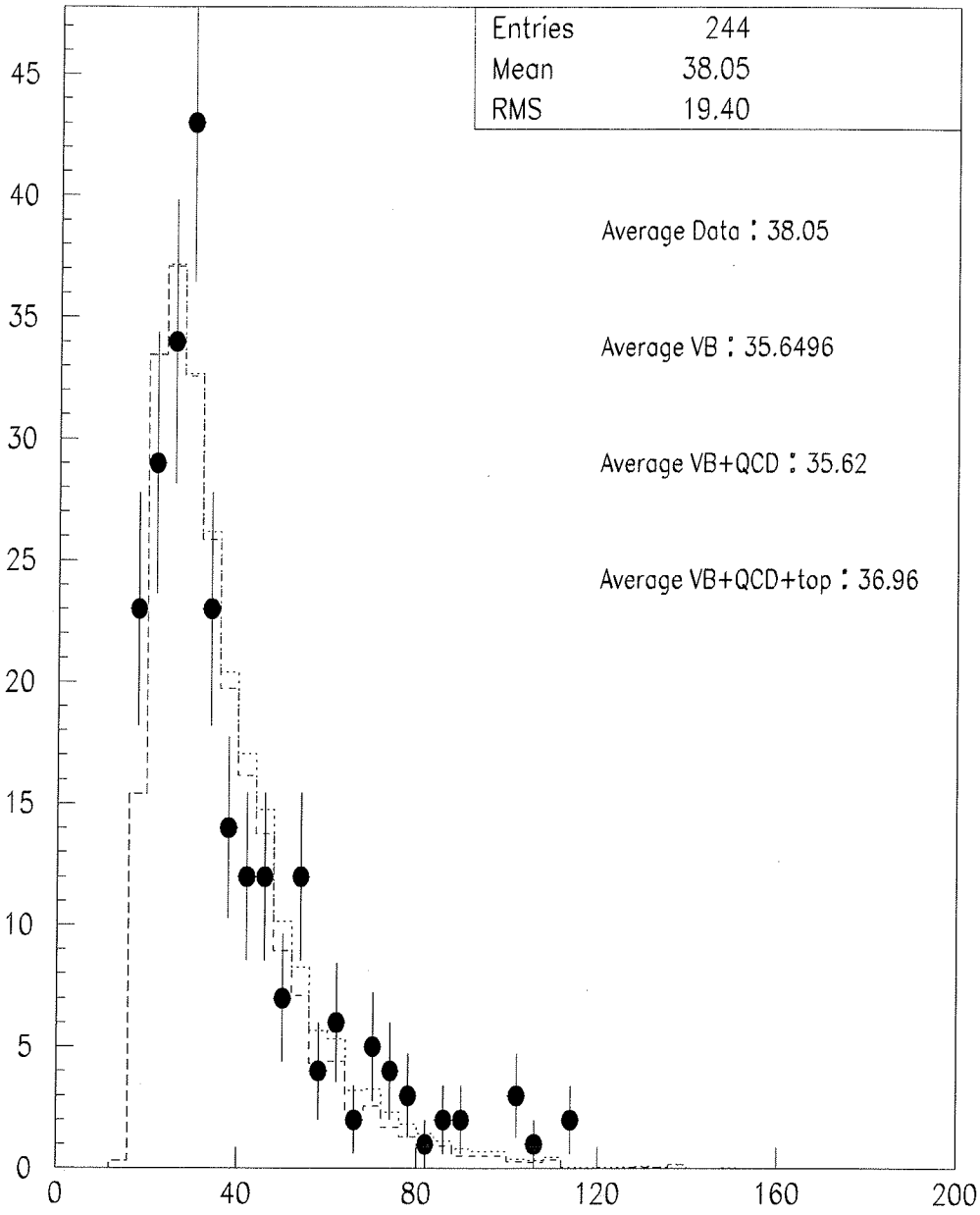

Figure 9: Comparison of H_T/jet distribution for Data and Monte Carlo, for $\geq$ 3jets.

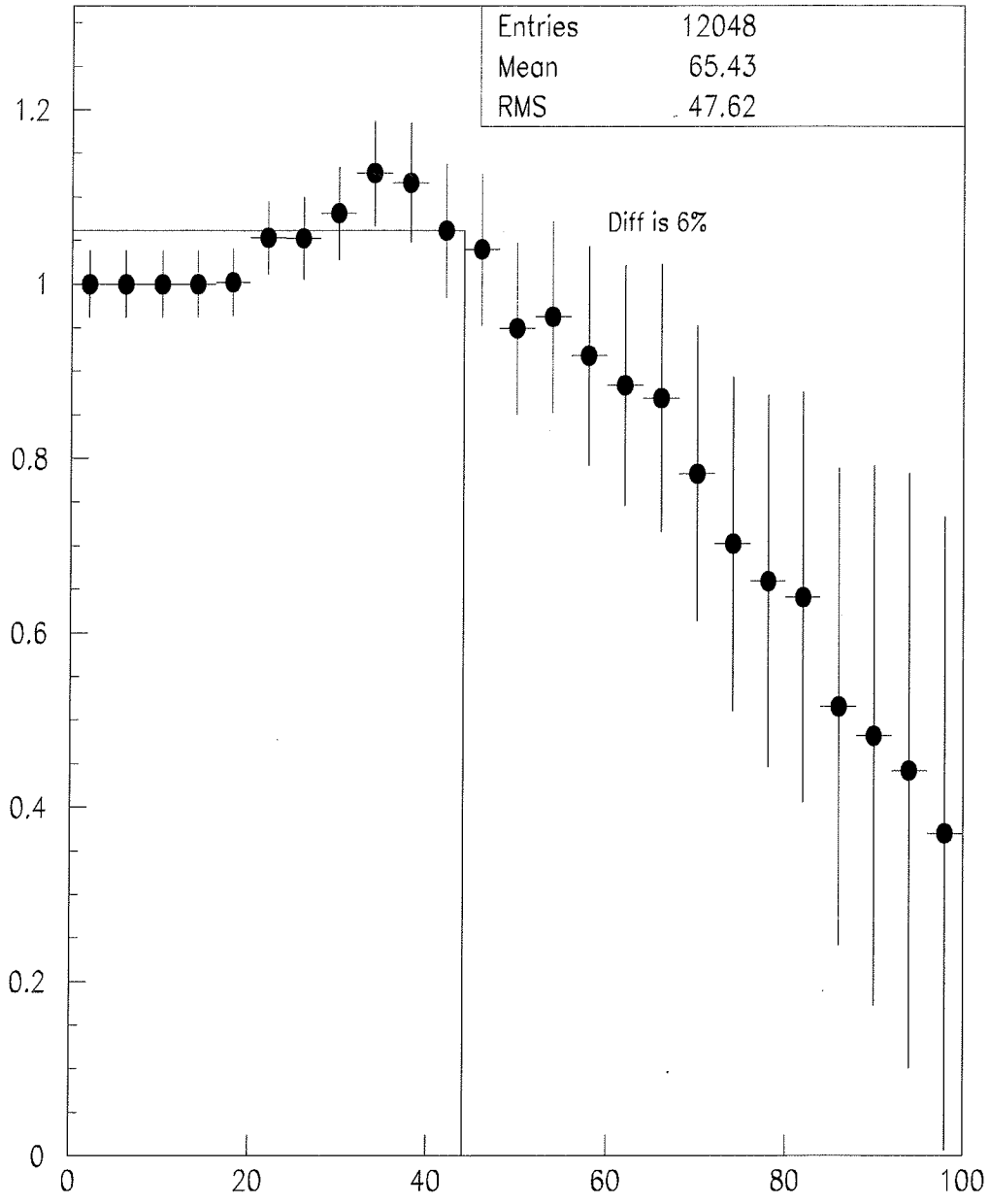

Figure 10: Ratio of # of events passing the H_T/jet cut for Data and Monte Carlo, for ≥ 2 jets

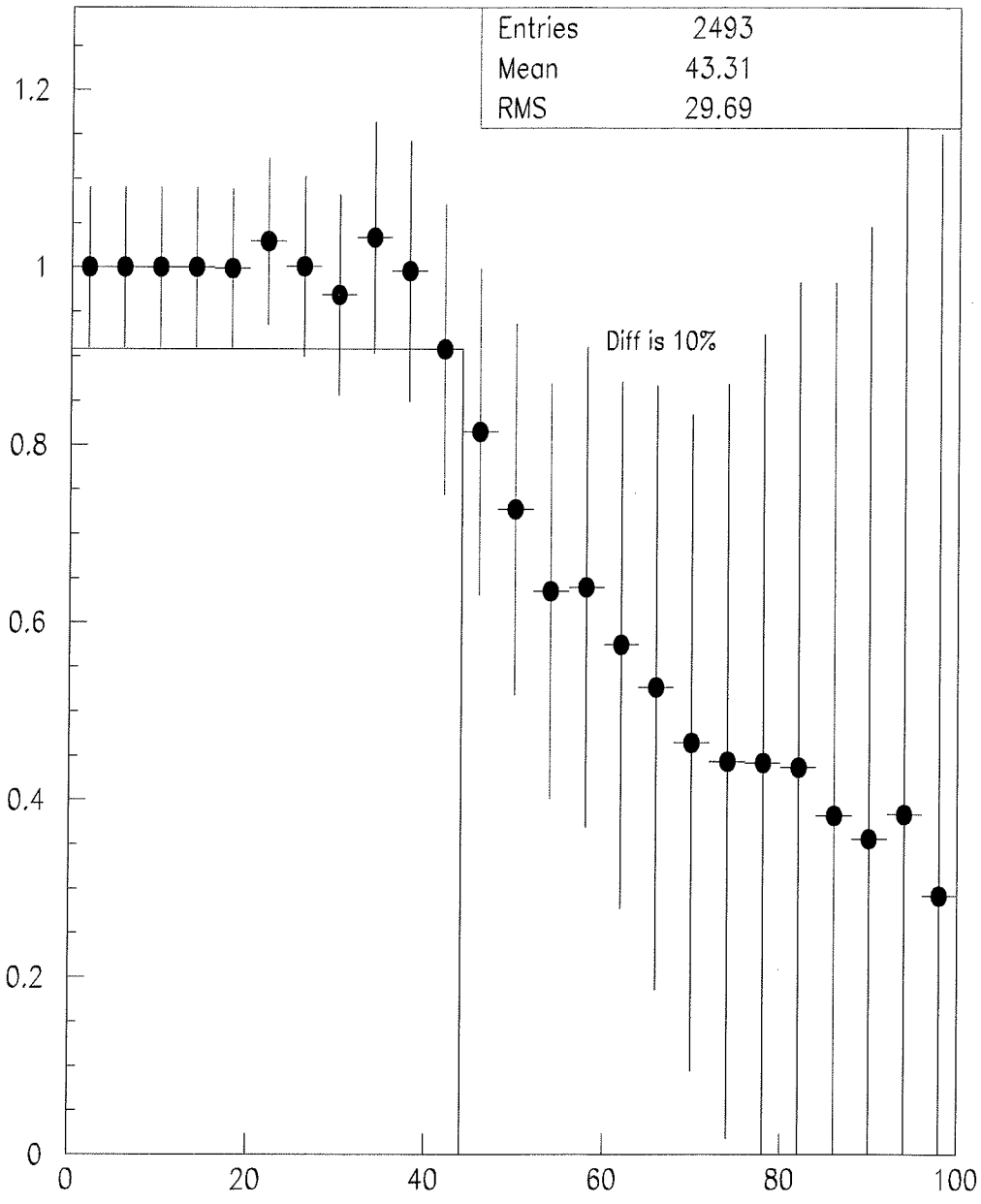

Figure 11: Ratio of # of events passing the H_T/jet cut for Data and Monte Carlo, for ≥ 3 jets

trigger efficiency.

The top yields listed in table 24 are computed using the standard model cross section for top production and corresponds to $\int \mathcal{L}dt = 105.9pb^{-1}$. This includes MAX_LIVE luminosities from both Run1A and Run1B which includes luminosity accumulated during Main Ring activity.

Table 24: $\epsilon * BR$ and $< N_{top} >$ for various top masses for "NS" cuts

M_{top} (GeV)	N_{tot}	N_{pass} All (CC ele, EC ele)	$\epsilon * BR$	$< N_{top} >$
140	29998	359 (358,1)	0.90 $\pm$0.22	16.1$\pm$4.0
160	29995	451 (428,23)	1.09 $\pm$0.24	9.5 $\pm$2.1
180	28995	582 (543,39)	1.45 $\pm$0.34	6.4 $\pm$1.6
200	29994	653 (610,43)	1.57 $\pm$0.35	3.5 $\pm$0.8

8.8 Systematic Error sources in Top acceptance

The sources of systematic error on Top acceptance, are listed in table 8.8.

Table 25: Systematic error sources in top accepatance determination for e+jets(μ-tag).

Source of uncertainity	% Error
Trigger Efficiency	1%
Eid efficiency	2%
Energy Scale	10%
Top Generator (Difference in ISAJET and HERWIG)	5%
Luminosity (Only for $< N_{top} >$)	5.4%

Here we determine Energy scale error by looking at the change in acceptance for different jet energy corrections(CAFIX Hi,Low and nominal) for different top masses(between 140GeV an 220 GeV). The mote carlo generator error was determined by looking at difference in acceptance for events

generated using ISAJET and HERWIG for same top mass(180 GeV and 200 Gev).

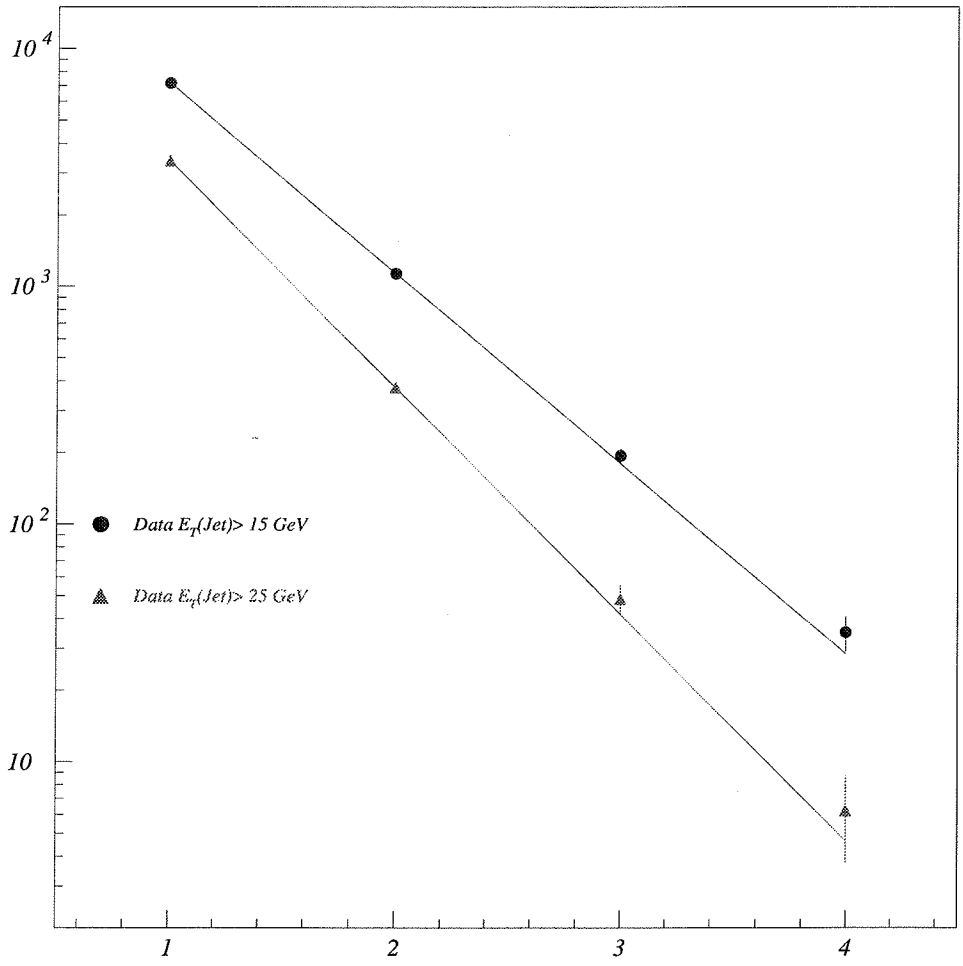

Figure 12: Inclusive Jet Multiplicity distribution (after QCD background subtraction) for Run1B data for two different jet E_T thresholds. Both the lines show the expected events with at least 3 and 4 jets events using the predicted exponential behaviour and our observation of number of events at the two lowest multiplicity points

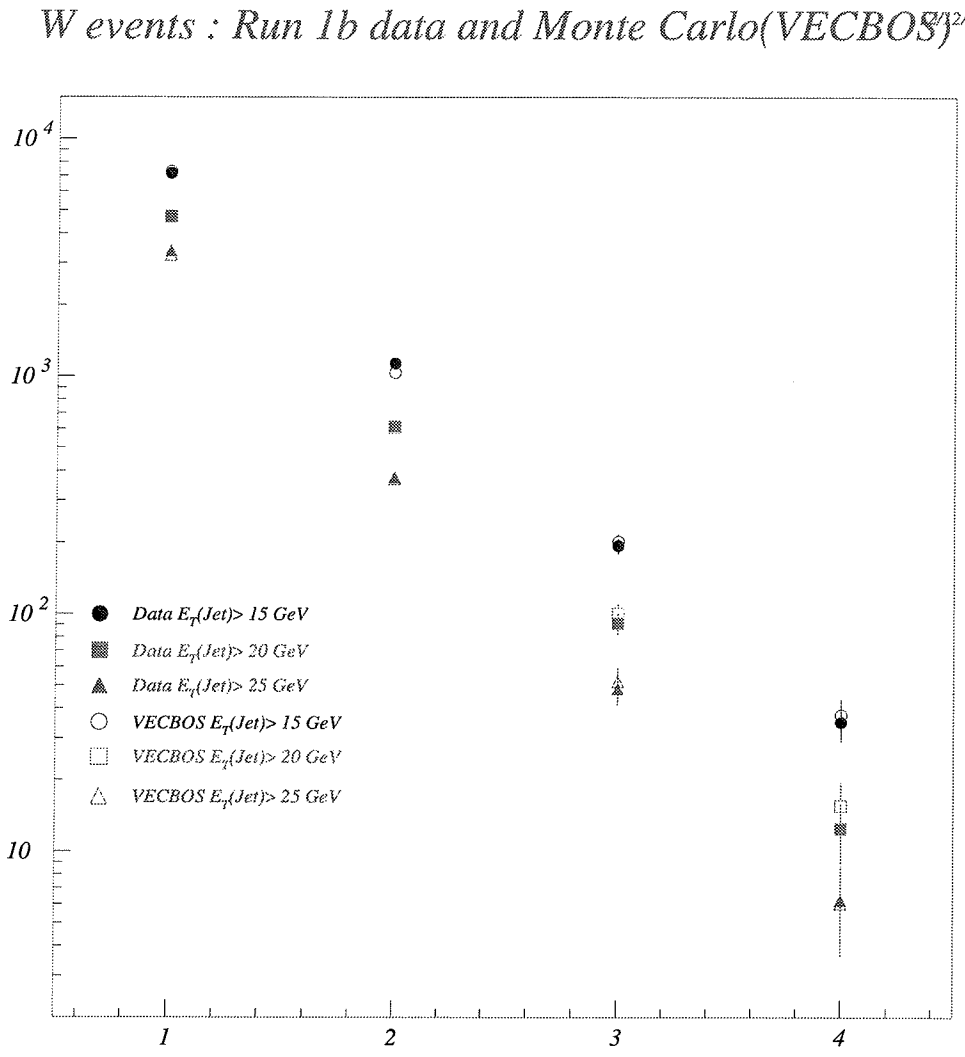

Figure 13: Inclusive Jet Multiplicity distribution (after QCD background subtraction) for Run1B data and those perdicted by VECBOS MC for three different jet E_T thresholds.

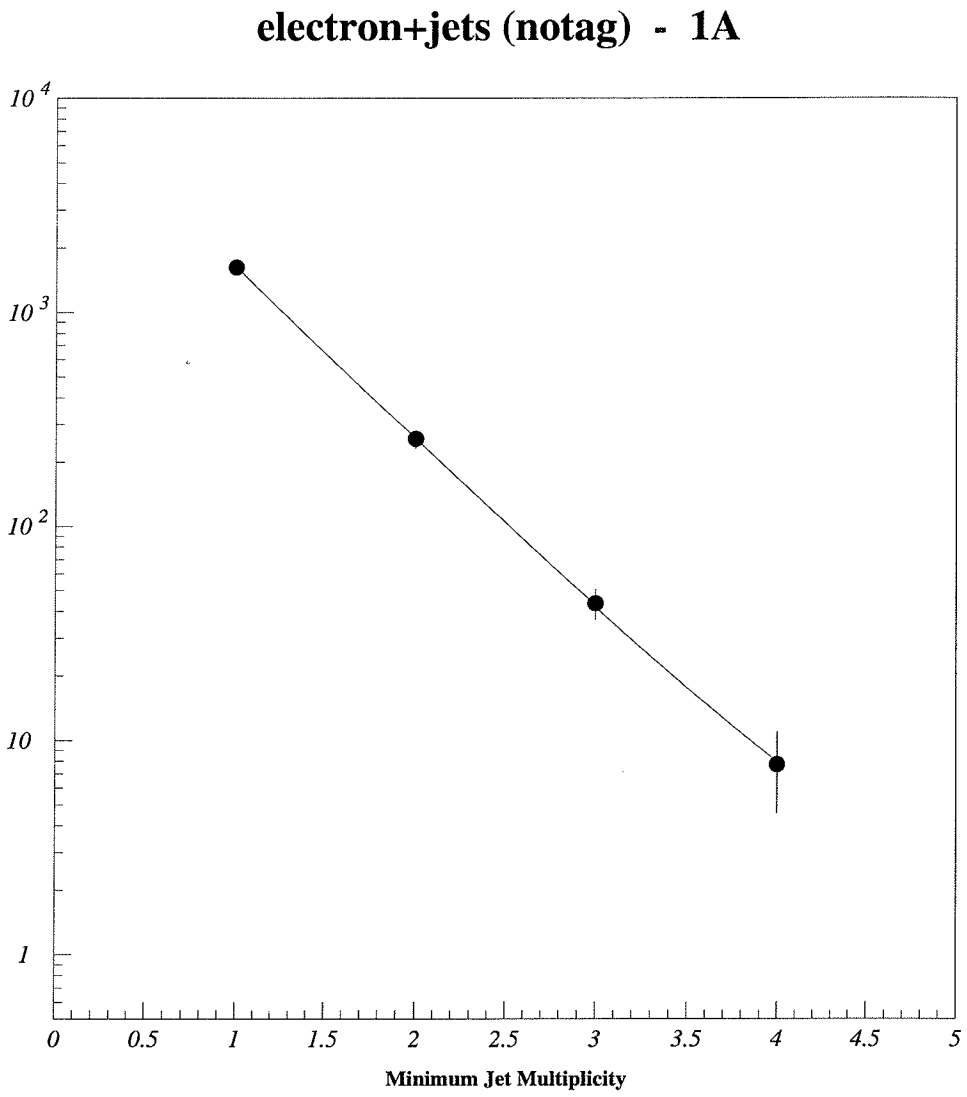

Figure 14: Inclusive Jet Multiplicity distribution (after QCD background subtraction and Berends fit to e+jets Run1A data sample

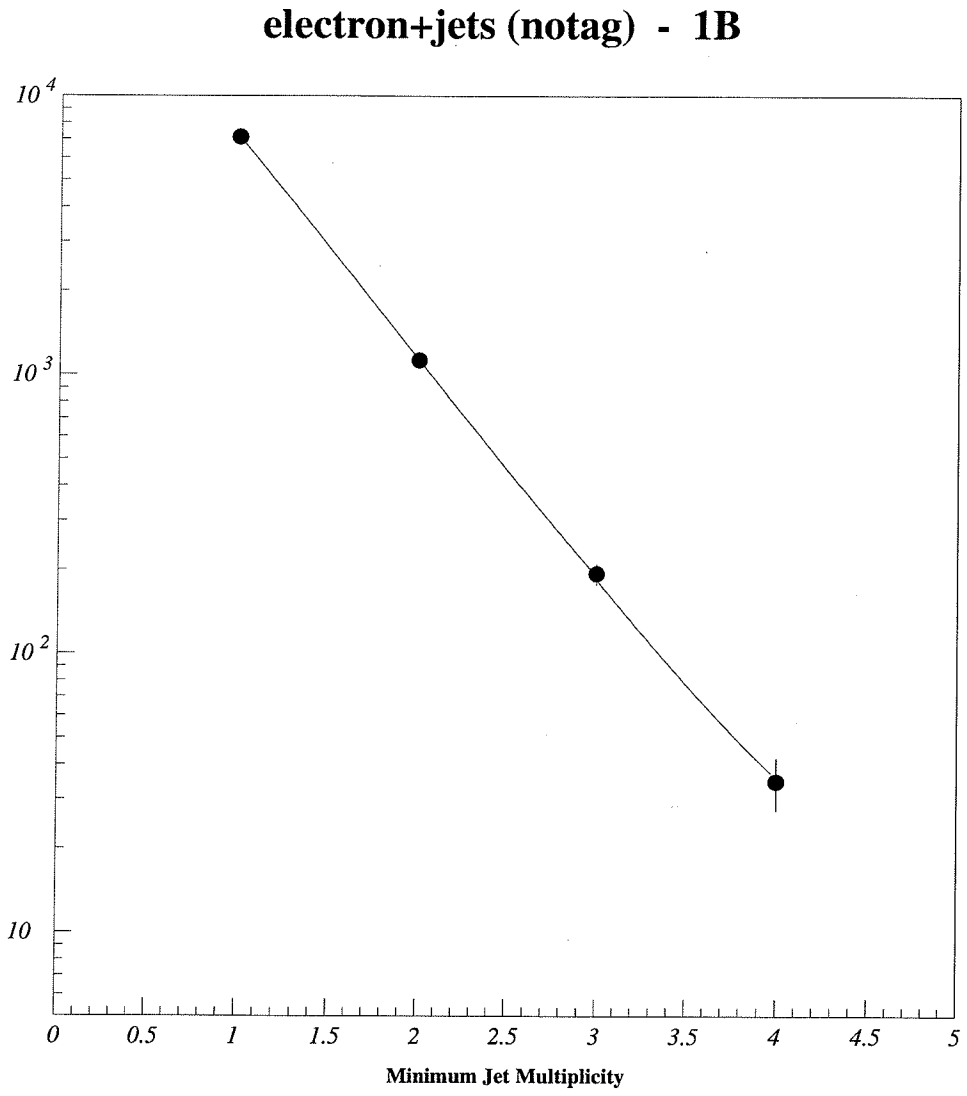

Figure 15: Inclusive Jet Multiplicity distribution (after QCD background subtraction and Berends fit to e+jets Run1B data sample

9 Muon+jets (noμ-tag) Analysis

From: SMTPTo: MEENA CC: Subj: Fixed up Aspen note. Changed pages also on your desk

Date: Fri, 24 May 1996 10:04:01 -0500 From: hobbs@d0sgi4.fnal.gov (John Hobbs) Message-Id: ¡199605241504.KAA19921@d0sgi4.fnal.gov¿ To: meena@fnald0.fnal.gov Subject: Fixed up Aspen note. Changed pages also on your desk

9.0.1 Selection Requirements

The selection requirements for the basic $t\bar{t} \rightarrow \mu +$ Jets analysis are

- *One* isolated muon and trigger (as above)
- Standard top group event cleanup
- $\not\!\!E_{\mathrm{T}}{}^{cal} \geq 20$ GeV
- $\not\!\!E_{\mathrm{T}} \geq 20$ GeV
- $\mathrm{N_{Jets}} \geq 4$, ($p_t \geq 15$ GeV, $|\eta| < 2.0$)
- no tag muon(s)

The cross-section or "standard" analysis also requires

- $E_T^W \geq 60$ GeV
- $A_W \geq 0.065$
- $H_T \geq 180$ GeV

Here E_T^W is the transverse energy of the μ and $\not\!\!E_{\mathrm{T}}$, A_W is the aplanarity calculated using all jets $p_t \geq 15$ GeV, $|\eta| < 2.0$ and H_T is the sum of the scalar energies of the jets used in computing A_W. Table 26 shows the number of events remaining as the analysis requirements are applied.[7] Tables 27

[7]Many of the detailed tables for the Ia data are not given explicitly in this section. T The missing tables can be found in appendix A.

and 28 give the candidate events for the ultra loose [8] and standard cuts for both $t\bar{t} \rightarrow \mu +$ Jets and $t\bar{t} \rightarrow \mu +$ Jets $+ \mu$(tag) channels. The first table is for Ia data. The second is for Ib data.

9.0.2 Multi-jet Background

The multi-jet (QCD) background at N jets is calculated by multiplying the number of $N+1$-jet non-isolated muon events satisfying all analysis requirements by the probability that a μ+jet system appears as an isolated muon. A non-isolated muon is a muon which satisfies all requirements for an isolated muon except that $\Delta R < 0.5$. Such events arise dominantly from $p\bar{p} \rightarrow q\bar{q}+X$ processes. The QCD background is calculated separately for the CF and EF for events passing a MU_JET_xxxx filter and events passing either a MU_JET_xxxx or JET_3_xxxx filter.

The false isolation probability for N jets is the ratio of the number of isolated muon events having N jets and $\not\!\!E_{\rm T} < 20$ GeV to the number of non-isolated muon events having N+1 jets and $\not\!\!E_{\rm T} < 20$ GeV. The results are shown in tables 29 to 32. The number of selected N+1 jet non-isolated muon events and the predicted QCD background is shown as a function of jet multiplicity in table 33.

9.0.3 W+jets Background

The W+jets background at four or more jets is computed using low jet-multiplicity W events and the hypothesis exponentially decreasing cross-section as a function of jet multiplicity. This can be formally expressed as $\sigma(W \rightarrow l\nu_l + Njets) = \sigma(W \rightarrow l\nu_l + 1jet) \times \alpha^{(N-1)}$. Here α is the exponential decay constant, and N is the number of jets. The number of four-jet $W \rightarrow \mu = nu$ events N_4^W is thus found using the expression

$$N_4^W = N_2^W \cdot \alpha^2$$

Here N_i^W is the number of i-jet W events. The decay constant α is estimated using the ratio N_2^W/N_1^W. The number of W plus one- and two-jet events are found by subtracting the QCD background at each multiplicity from

[8] The ultra-loose cuts are identical to the basic requirement except that the jet counting includes jets satisfying the looser requirement $|\eta| \leq 2.5$.

Requirement	Number of Events			
	Ia		Ib	
	CF	EF	CF	EF
—	2009	407	9526	3609
MU_JET_xxxx	1104	133	6092	1834
Clean up	1096	132	6068	1831
$\not\!\!E_{\rm T}$>20 GeV	494	46	3097	473
$\not\!\!E_{\rm T}$>20 GeV	274	23	1970	278
$N_J \geq 1$	274	23	1970	278
$N_J \geq 2$	88	8	490	93
$N_J \geq 3$	15	2	112	24
$N_J \geq 4$	4	1	26(3)	6(0)
E_T^W	3	1	20(3)	6
$A_W > 0.065$	2	1	11(2)	3
$H_T \geq 180$ GeV	2	1	4(1)	0
All filters	—	—	31	20
$N_J \geq 4$	—	—	31(3)	20(0)
E_T^W	—	—	25(3)	18
$A_W > 0.065$	—	—	15(2)	5
$H_T \geq 180$ GeV	—	—	7(1)	0

Table 26: Number of events passing analysis requirements. The initial selection requirement is one isolated muon, at least one jet ($|\eta| < 2.0, p_t >$ 15 GeV), no tag muons and GOOD_BEAM. The number in parentheses is number of additional events coming from the MRBS_LOSS periods. There was no $\not\!\!E_{\rm T}$ based filter for the Ia analysis.

Run	Event	Standard	Tag	MRBS
58203	4980	X	X	
61275	9188	X		
61514	4537			
62953	2932			
63183	13926	X		
63740	14197	X		

Table 27: The list of Ia candidate events for the $t\bar{t} \rightarrow \mu +$ Jets and $t\bar{t} \rightarrow \mu +$ Jets $+ \mu$(tag) analyses. All events not marked as "Standard" pass the top group ultra loose requirement of at least four jets having $|\eta| < 2.5$ and $p_t > 15$ GeV.

the number of observed events and multiplying the difference by a trigger correction, and only events with CF muons selected using the MU_JET_xxxx triggers are used in this the exponential scaling calculation.

The trigger correction is needed because the trigger efficiency depends on the number of jets for low multiplicity events. Table 34 shows the trigger bias as a function of multiplicity. The bias is calculated by comparing the number of events selected using a muon-only trigger with the number passing both the muon-only trigger and the MU_JET_xxxx triggers as a function of multiplicity. The events are required to pass all other analysis cuts.

The number of observed events, QCD background and number of W+jet events are shown as a function of jet multiplicity in table 35 and for Ib in table 36. For the Ib data, $\alpha = 0.21 \pm 0.02$. For Ia, $\alpha = 0.25 \pm 0.04$. These errors are statistical only. Figure 16 shows the exponential fall-off of cross section with jet multiplicity for simulated W events, and figure 17 shows the same quantity for QCD subtracted data. The curves also illustrate the effect of jet thresholds on the α parameter.

The resulting W+4 jet background is then corrected by 1.5 as described above to account for the additonal trigger efficiency of the JET_3_xxxx triggers and the additional acceptance provided by the EF region. This then gives the total W+jets background for the basic analysis. The result is given in table 39.

Run	Event	Standard	Tag	MRBS
77304	8028			
78121	2325			
80703	31477			
80887	5976			
81909	11966	X		X
82639	11573			
82694	25595	X		
83074	22558			
84470	32527			
84492	22977			
84534	15306			
84695	29699	X	X	
84696	29253	X		
85888	28599	X		
85915	24726			
86072	8462	X	X	
87063	14368			
87329	8787			
87448	3192			
87820	6196			
87880	18470			
88464	2832			
88530	7800			
88597	1145			
88603	2131			
89452	1810			
89463	14233			
89681	3196			
89706	13481			
89751	27345			
89943	19016			

Table 28: The list of Ib candidate events for the $t\bar{t} \rightarrow \mu +$ Jets and $t\bar{t} \rightarrow \mu +$ Jets $+ \mu$(tag) analyses. All events not marked as "Standard" pass the top group ultra loose requirement of at least four jets having $|\eta| < 2.5$ and $p_t > 15$ GeV.